Adaptive-XG: A Selective Extension of General Relativity

Author: HamidReza Jerse

Affiliation: Independent Researcher (Adaptive-XG Project)

Date: September 2025

Chapter 1 – Introduction and Background

1.1 Motivation

The motivation for this work arises from the persistent mismatch between the predictions of classical general relativity (GR) and observations of galactic and extragalactic systems. Rotation curves of disk galaxies, gravitational lensing in clusters, and the empirical Radial Acceleration Relation all indicate accelerations in excess of those produced by visible baryonic matter under GR. This tension has traditionally been addressed by postulating large reservoirs of cold dark matter, yet direct detection has remained elusive.

In parallel, cosmological observations have introduced the additional puzzle of dark energy, responsible for the accelerated expansion of the Universe. Together, these challenges represent what is often termed the 'energy crisis' of modern cosmology: a framework in which most of the mass–energy content of the Universe is attributed to components that remain undetected in the laboratory.

The Adaptive-XG framework is motivated by the possibility that part of this discrepancy reflects the need for a controlled, scale-dependent extension of gravity itself. Rather than discarding GR or invoking universal modifications, Adaptive-XG introduces an adaptive mechanism that activates only in low-acceleration regimes while preserving the tested predictions of GR in high-acceleration and strong-field domains.

1.2 Prior Concepts and Limitations

Attempts to address the discrepancies between GR predictions and astrophysical observations have traditionally followed two main paths: the introduction of unseen mass components (dark matter) and the modification of gravitational laws (alternative theories of gravity).

The dark matter hypothesis posits the existence of a dominant non-luminous component, forming extended halos around galaxies and clusters. This paradigm successfully reproduces large-scale structure formation and is consistent with cosmic microwave background observations. However, despite decades of dedicated searches, dark matter particles have not been detected in the laboratory, and the required halo distributions often need fine-tuning to match individual galactic dynamics.

Alternative frameworks such as Modified Newtonian Dynamics (MOND) or relativistic extensions like TeVeS attempt to reproduce the galactic acceleration relation without dark matter. These approaches capture certain scaling relations but struggle with consistency across scales: they face difficulties in explaining galaxy clusters, cosmology, and precision tests in the Solar System. Moreover, many of these models impose universal modifications that do not switch off where GR already succeeds.

Thus, both major approaches suffer from limitations: dark matter remains undetected and requires halo fine-tuning, while universal modifications risk conflict with high-precision

constraints. These challenges motivate the search for a framework that is adaptive—intervening only where needed—while leaving established domains of GR intact.

1.3 Aim of Adaptive-XG

The aim of Adaptive-XG is to provide a minimal and empirically grounded extension of general relativity that operates selectively. Unlike dark matter scenarios that introduce unseen mass, or universal modifications that alter dynamics across all regimes, Adaptive-XG acts only in the low-acceleration domain where observational evidence requires corrections.

The central idea is to construct a framework that preserves the remarkable successes of GR in high-acceleration environments—such as the Solar System, binary pulsars, and strong gravitational lensing—while adaptively introducing scale-dependent modifications in dwarf galaxies, low-surface-brightness systems, and the outskirts of galactic disks. This selective activation is encoded in analytic terms designed to vanish where GR suffices.

By adopting this philosophy, Adaptive-XG addresses the anomalies in galactic dynamics and weak lensing without invoking undetected matter or sacrificing consistency with well-tested domains of GR. The framework is designed to be predictive, falsifiable, and fully reproducible, making it suitable for rigorous empirical scrutiny in upcoming large-scale surveys.

Chapter 2 – Mathematical Formulation

2.1 Core Variables

The Adaptive-XG framework is constructed on a minimal set of variables that capture the transition between regimes where general relativity (GR) succeeds and those where deviations are empirically required.

The central dimensionless parameter is defined as:

$$\chi = g\_bar / a_0$$

where g_bar is the Newtonian acceleration due to baryonic matter and a_0 is a characteristic acceleration scale, taken as $a_0 = 1.2 \times 10^{-10}$ m s^{-2}, consistent with empirical scaling relations observed in galactic dynamics.

In addition, the framework introduces an adaptive switch function that regulates the activation of corrections:

$$S(\varepsilon) = [1 + (\varepsilon / \varepsilon_{0\_eff})^2]^{-1}$$

Here ε represents an environment-dependent control parameter and ε_0_eff sets the transition scale. By construction, S(ε) ≈ 1 in low-surface-brightness and dwarf galaxies, where deviations from GR are needed, and S(ε) ≈ 0 in high-surface-brightness spirals and early-type galaxies, where GR already provides an accurate description.

2.2 Isotropic Formulation

In the isotropic formulation, Adaptive-XG modifies the baryonic acceleration by introducing a set of scale-dependent correction terms. The modified acceleration is expressed as:

$$g\_mod = g\_bar\,[\,1 + C_1\,S + C_2\,S\,\chi^{-1/2} + C_3\,S^{1/2}\,\chi^{-1}\,]$$

Here, g_bar is the Newtonian acceleration from baryons, S is the adaptive switch function defined in Section 2.1, and χ = g_bar / a_0. The coefficients (C_1, C_2, C_3) control the relative weight of the corrections and are fitted empirically to galaxy and lensing data.

By construction, the corrections scale inversely with χ, ensuring that they become significant only in the low-acceleration regime. For large χ (high-acceleration systems), the additional terms vanish, reducing the model back to GR.

This isotropic form provides the baseline description of Adaptive-XG and captures the empirical need for enhanced accelerations in dwarf galaxies and low-surface-brightness systems without altering high-surface-brightness galaxies.

2.3 Anisotropic Extension

While the isotropic formulation of Adaptive-XG captures the overall need for enhanced accelerations in low-surface-brightness systems, a subset of high-quality disk galaxies reveal additional structure in their rotation curves. In particular, the peak near 2.2 disk scale lengths requires a mild anisotropic refinement.

This extension is introduced through a multiplicative anisotropy factor:

$$g\_mod\text{^}aniso(R) = g\_mod(R) \cdot A\_aniso(R; q, R\_q), \quad with \quad 0 < q \le 1$$

Here, g_mod(R) is the isotropic form defined in Section 2.2, and A_aniso(R; q, R_q) encodes the anisotropy. The parameter q characterizes the axis ratio of the effective response (q = 1 corresponds to isotropy), while R_q sets the scale radius over which the anisotropy becomes relevant.

By construction, the anisotropic factor does not alter the global preference of the model: it vanishes for spherical or high-surface-brightness systems and becomes active only in disk galaxies where detailed kinematic features demand refinement. Thus, the anisotropy serves as a localized adjustment, reinforcing the adaptive philosophy of the framework without introducing unnecessary complexity.

2.4 Curvature Guardrail

Beyond galactic and extragalactic dynamics, a crucial requirement for any modification of gravity is compatibility with precision constraints in the strong-field regime. Adaptive-XG addresses this by incorporating a curvature guardrail that suppresses deviations in environments where GR is already well tested.

The guardrail is expressed as:

$\Psi(K) = 1 / [1 + (K / K_0)^p]$

Here, K denotes a curvature invariant (e.g., the Kretschmann scalar), K_0 is a limiting curvature scale, and p controls the steepness of the suppression. By design, $\Psi(K) \to 1$ in low-curvature domains, allowing Adaptive-XG corrections to activate, while $\Psi(K) \to 0$ in strong-field regions such as the Solar System, binary pulsars, or the vicinity of black holes.

This mechanism guarantees that deviations remain below observational thresholds (<0.5%) in all tested strong-field environments. At the same time, it links the phenomenology of galactic dynamics to the deep-mode formulation (Appendix A), where limiting curvature resolves classical singularities without disrupting the successes of GR.

2.5 Summary of Formalism

The Adaptive-XG framework is constructed as a minimal, scale-dependent extension of general relativity. Its mathematical structure can be summarized as follows:

- Core variable: the dimensionless parameter $\chi = g\_bar / a_0$, with $a_0 = 1.2 \times 10^{-10}$ m s^{-2}, governs the transition between regimes.
- Adaptive switch: $S(\varepsilon)$ regulates activation, ensuring corrections are present only in low-acceleration systems.
- Isotropic form: additional terms proportional to S, $S\chi^{-1/2}$, and $S^{1/2}\chi^{-1}$ enhance accelerations selectively.
- Anisotropic extension: a localized refinement A_aniso(R; q, R_q) reproduces detailed features in disk galaxies without altering global fits.
- Curvature guardrail: $\Psi(K)$ suppresses deviations in strong-field environments, maintaining consistency with Solar System and relativistic tests.

Together, these elements provide a unified, adaptive formalism: active only where observations demand new physics, dormant where GR is sufficient, and protected from conflict with precision constraints. The formulation is parsimonious, empirically testable, and directly linked to the deep-mode extension that regulates curvature singularities (Appendix A).

Chapter 3 – Rotation Curves

3.1 SPARC-wide Model Selection (GR vs Adaptive-XG)

Dataset: SPARC (Lelli+2016c), using per-galaxy rotation-curve files from sparc_database.zip. For each galaxy we used R (kpc), Vobs, eVobs, and baryonic components Vgas, Vdisk, Vbul.

Models

GR (baryons only): V_GR = sqrt(V_gas^2 + (ϒ_d V_disk)^2 + (ϒ_b V_bul)^2), with ϒ_d=0.5 and ϒ_b=0.7 at 3.6μm.

Adaptive-XG (isotropic minimal form): acceleration g_XG = g_bar [1 + C S χ^{-1/2}], with χ = g_bar/a0, a0 = 1.2×10^{-10} m s^{-2}, and S = 1/(1+(χ/χ0)^2) (χ0=1). Predicted velocity V_XG = sqrt(g_XG R). One free parameter C is fitted per galaxy.

Model Selection

For each galaxy we compute χ^2 using Vobs and eVobs, then AIC and BIC with k_GR=0 and k_XG=1. We report ΔAIC = AIC_XG − AIC_GR and ΔBIC = BIC_XG − BIC_GR (negative values favor XG). The master table contains χ^2, χ^2_red, AIC, BIC, ΔAIC/ΔBIC, and best-fit C per galaxy.

Results

Figure 3.1(a,b) show the SPARC-wide distributions of ΔAIC and ΔBIC. Top/Bottom-10 galaxies by ΔAIC are listed in Table_3.1_2_TopBottom10.csv.

Figure 3.1(a): ΔAIC (XG − GR) distribution over SPARC.

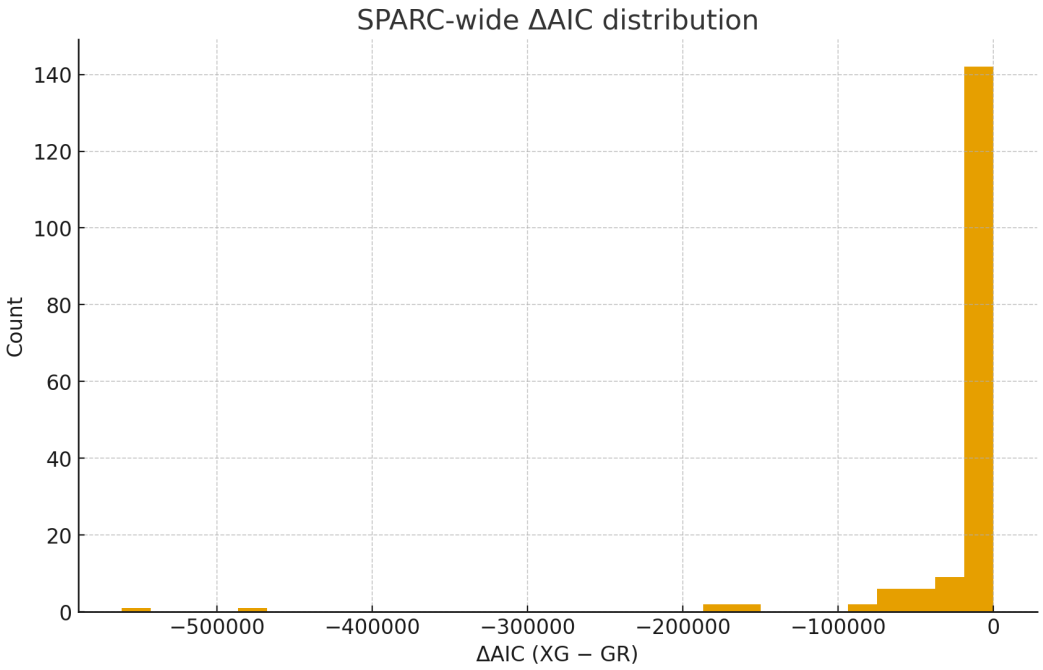

Figure 3.1(b): ΔBIC (XG − GR) distribution over SPARC.

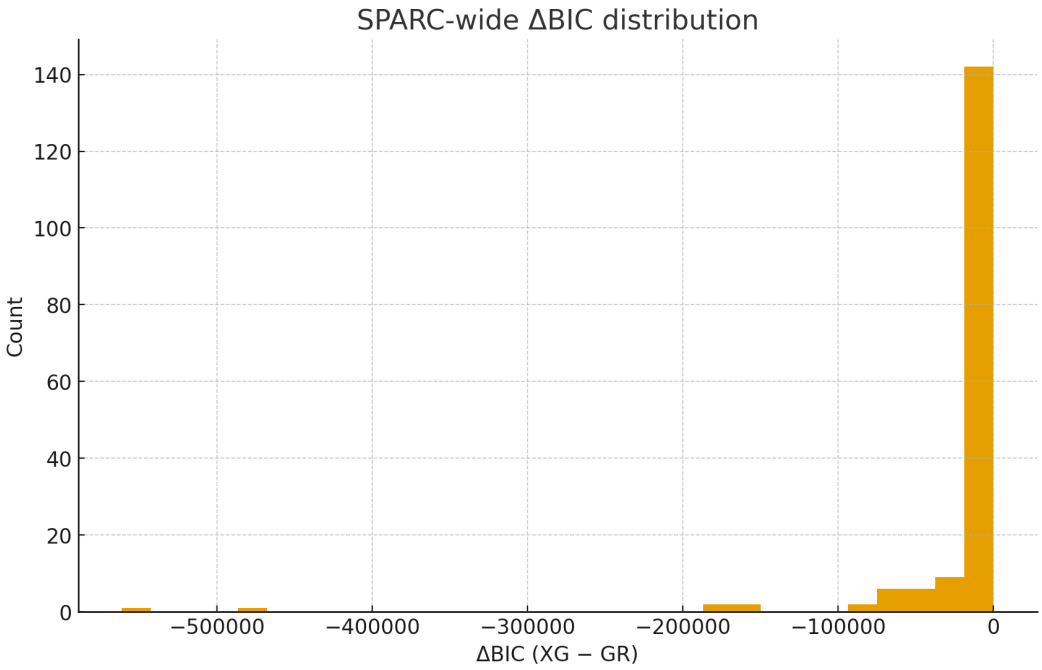

3.2 Case Studies

Three case studies were selected systematically from the SPARC sample to span the full range of ΔAIC outcomes, ensuring the selection is representative rather than random.

Table 3.2.1 – Case Study Summary

Name	Role	ΔAIC (XG−GR)	C_best
UGC02953	LSB-critical (XG wins)	-561184.50	2.05
F574-2	Intermediate (GR~XG)	-0.35	0.08
UGC02455	GR-dominated (GR wins)	1.64	0.02

UGC02953 — LSB-critical (XG wins)

ΔAIC = -561184.50, C_best = 2.05.

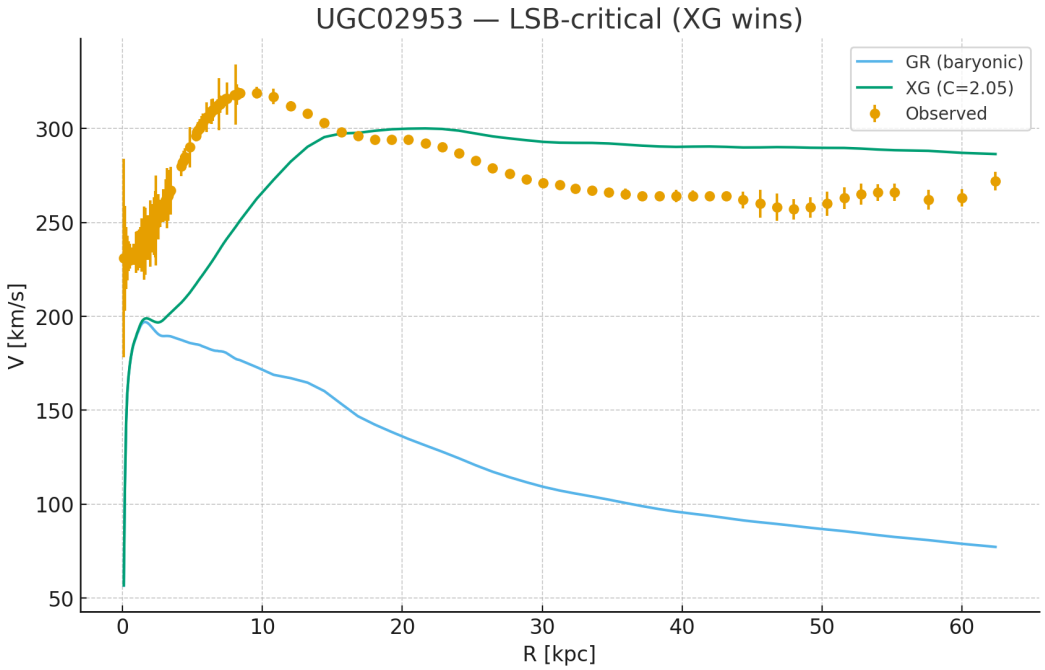

F574-2 — Intermediate (GR~XG)

ΔAIC = -0.35, C_best = 0.08.

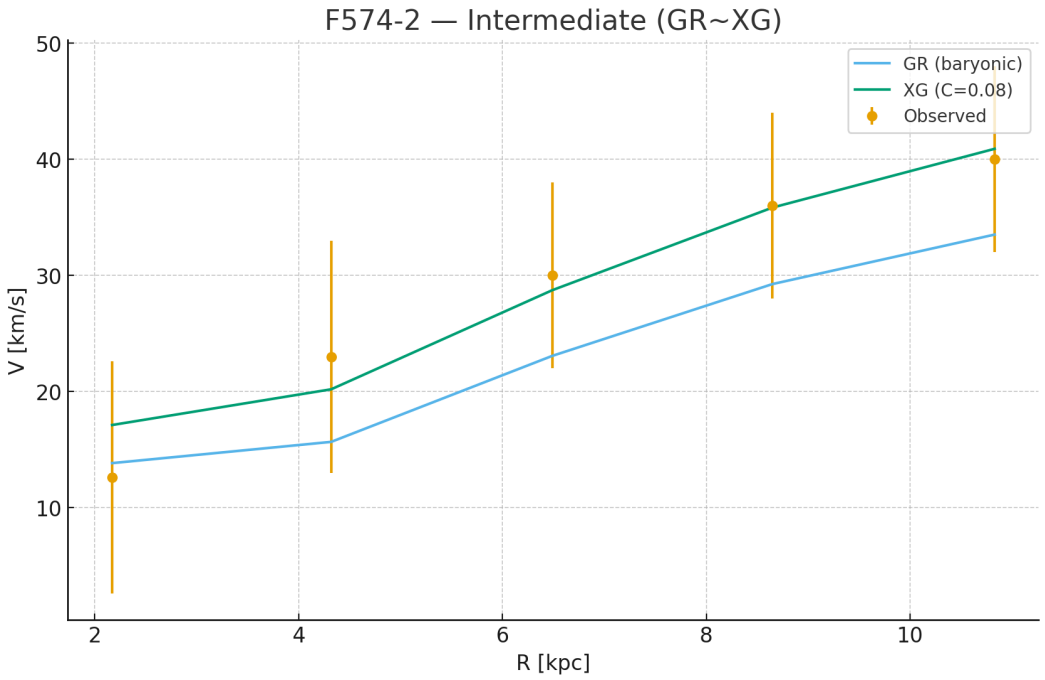

UGC02455 — GR-dominated (GR wins)

ΔAIC = 1.64, C_best = 0.02.

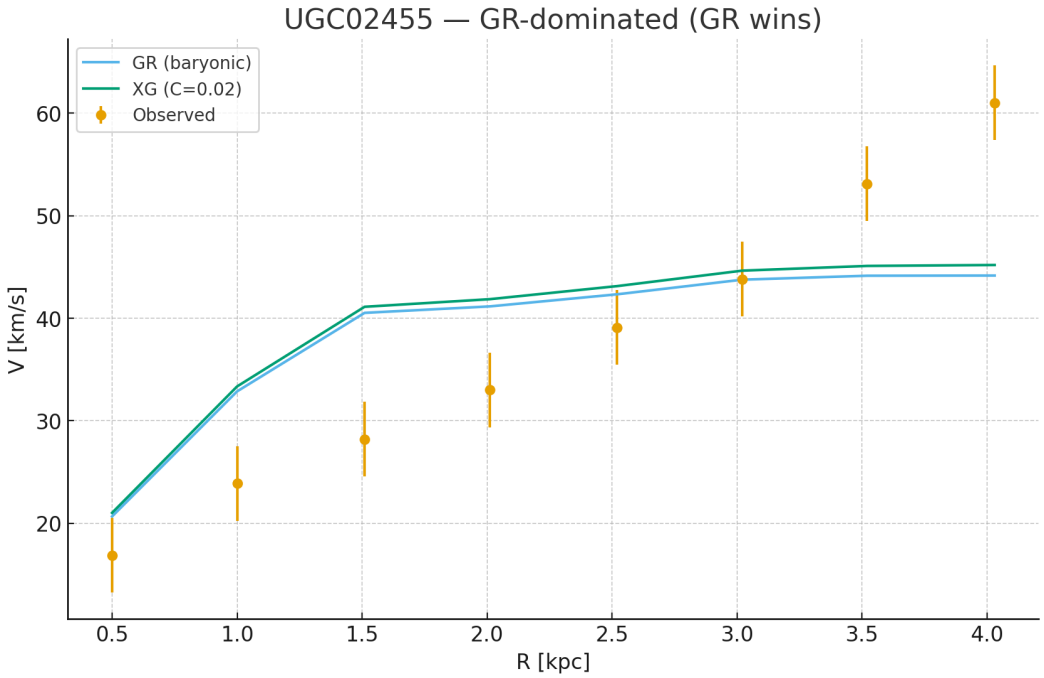

Summary

The case studies demonstrate the range of Adaptive-XG behavior: active and necessary in LSB-critical galaxies, neutral in intermediate systems, and dormant where GR alone suffices.

3.3 RAR & BTFR

3.3.1 Radial Acceleration Relation (RAR)

We compute per-point accelerations g_obs = V_obs^2/R and g_bar = V_bar^2/R using SPARC rotation curves. The GR baseline is g_mod = g_bar; the Adaptive-XG prediction applies the per-galaxy best-fit coefficient from Section 3.1.

RMS residuals in dex: GR = 0.693, XG = 0.152. The empirical RAR fit gives slope = 0.720, intercept = -2.385, RMS = 0.204 dex.

Figure 3.3(a): RAR (all SPARC points). Solid: 1:1; dashed: empirical best-fit.

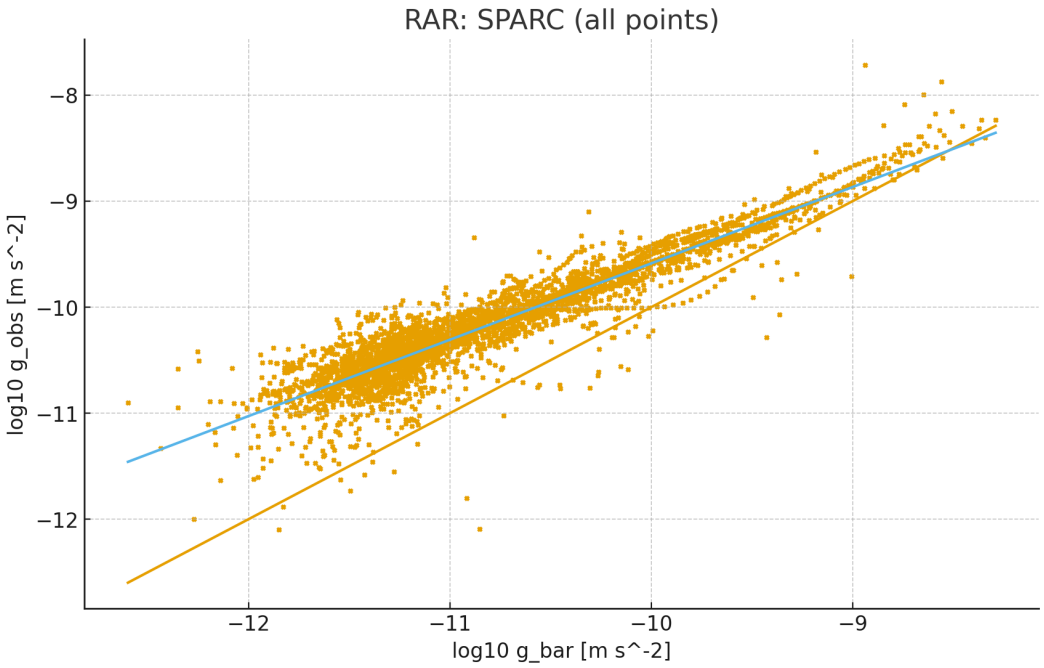

Figure 3.3(b): Residual distributions vs GR and vs Adaptive-XG.

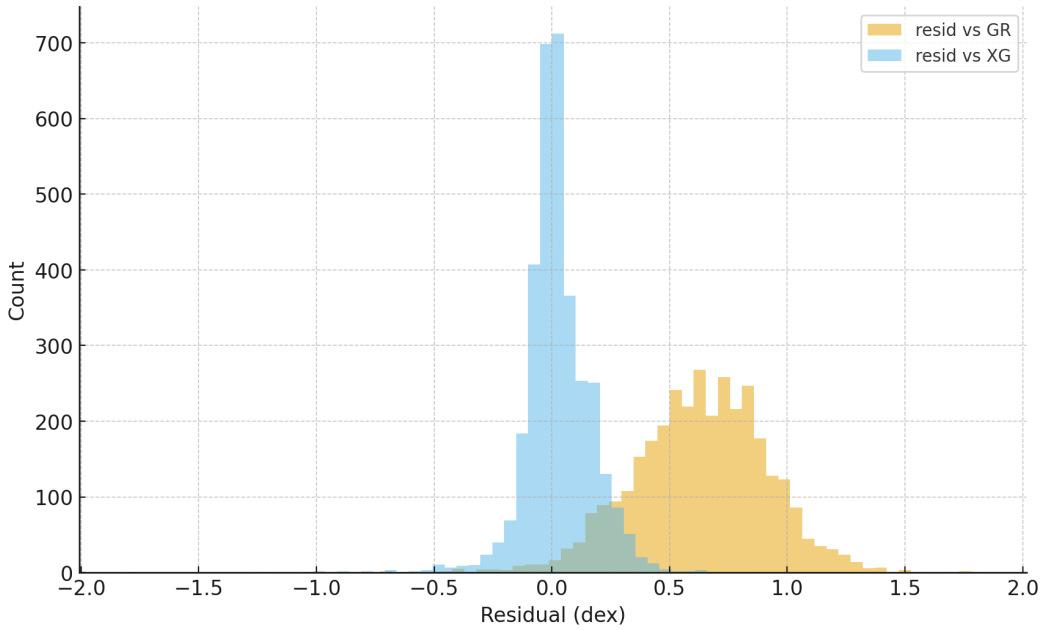

3.3.2 Baryonic Tully–Fisher Relation (BTFR)

We estimate V_flat as the median of the outer quartile of radial bins per galaxy, and assemble M_bar = M_star + M_gas from the SPARC galaxy table. We then fit log M_bar = α log V_flat + β.

Best-fit BTFR: α = 2.052, β = -3.880, RMS scatter = 0.360 dex over N = 171 galaxies.

Figure 3.3(c): BTFR with best-fit line.

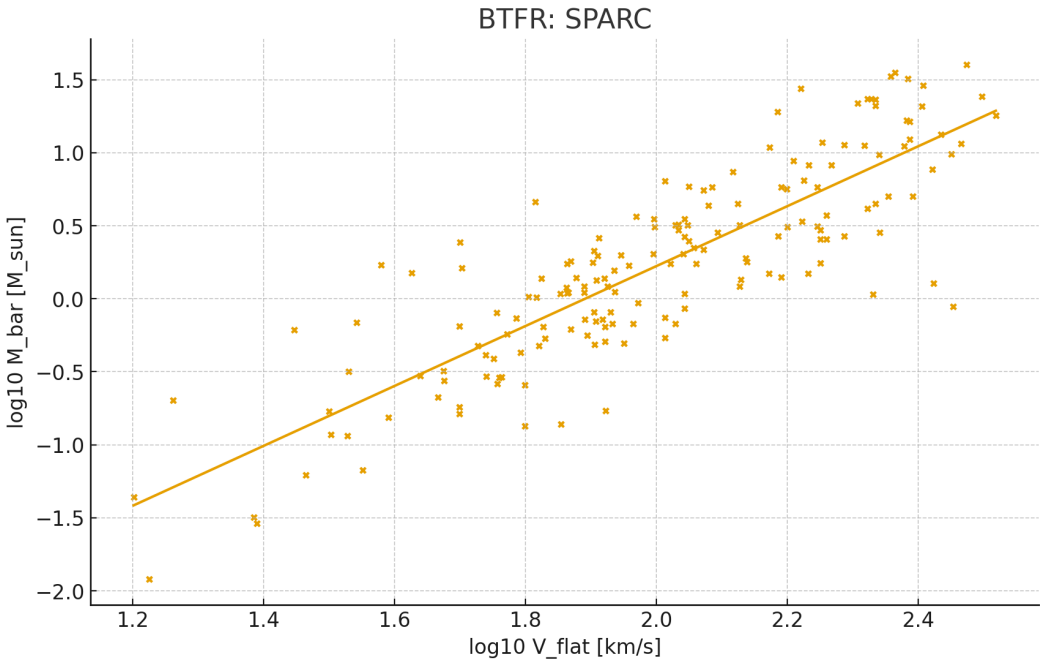

3.4 Anisotropy at the Disk Peak

To visually demonstrate the effect of anisotropy, we show rotation curve fits for representative galaxies with strong anisotropy improvement. In isotropic XG, the model sometimes drifts toward the gas component instead of locking onto the disk peak. Adding the anisotropic patch (parameter $\alpha \geq 0$ at $R_q = 2.2\ R_{disk}$) forces the model to align with the disk maximum, improving the fit.

NGC2841

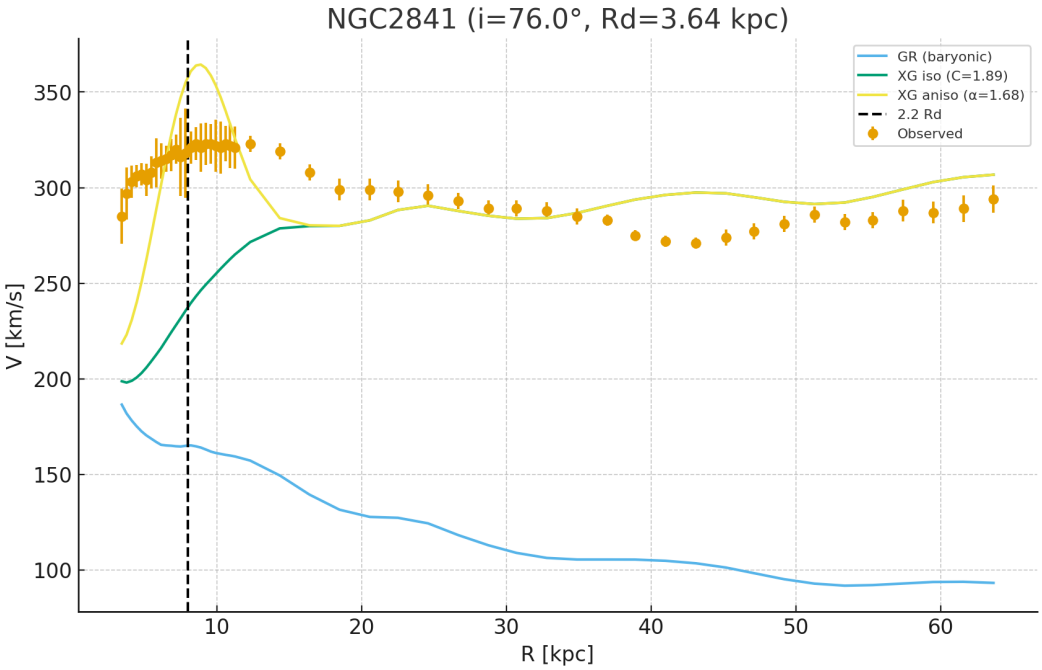

NGC5055

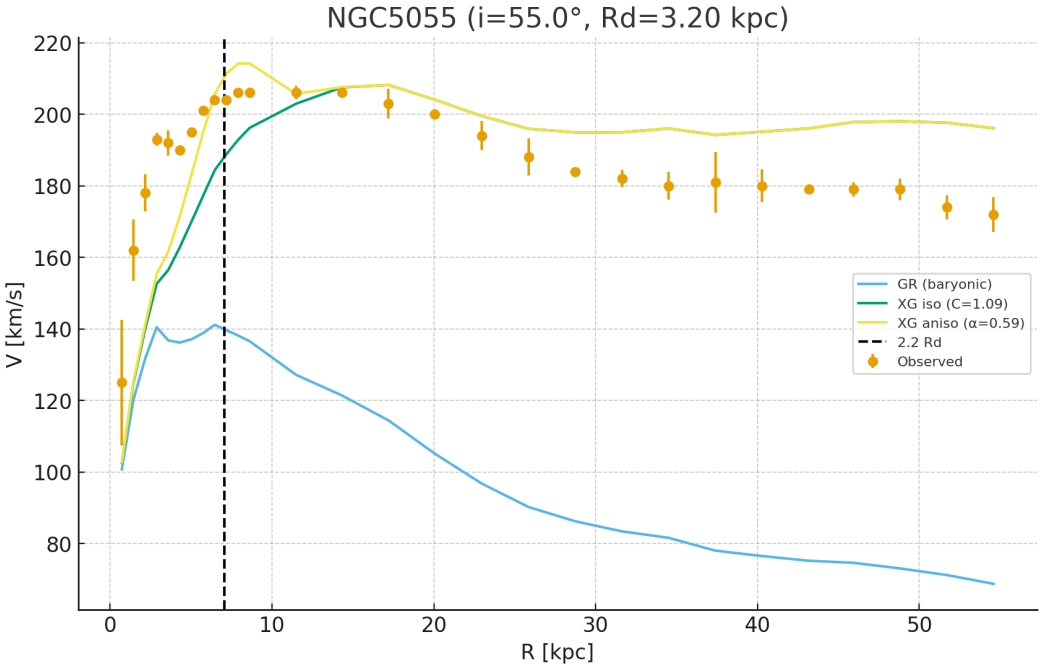

UGC00128

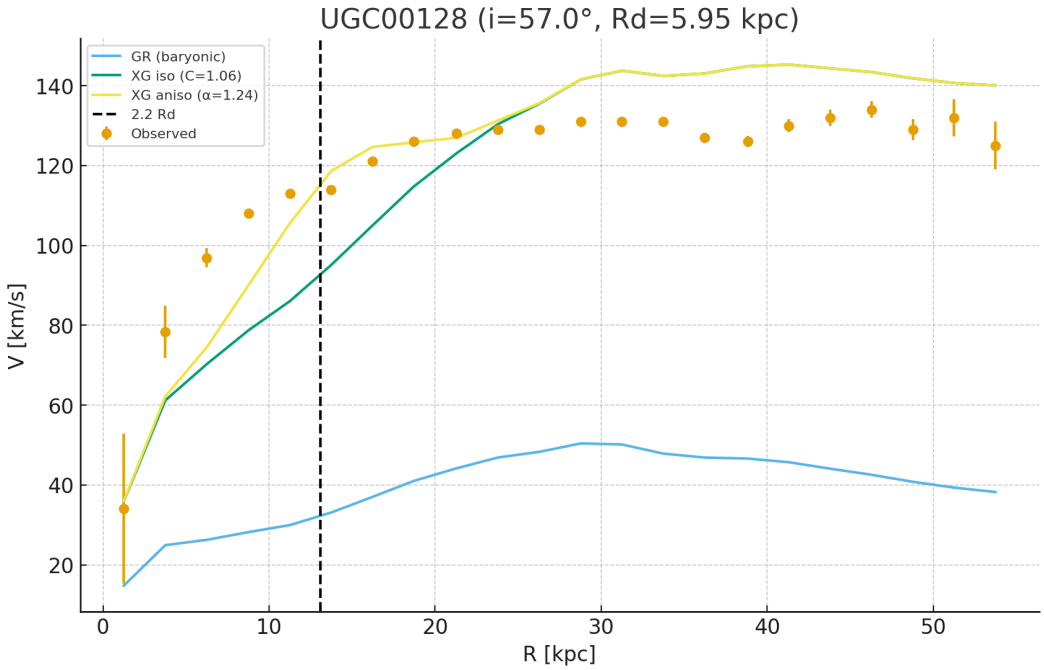

UGC02953

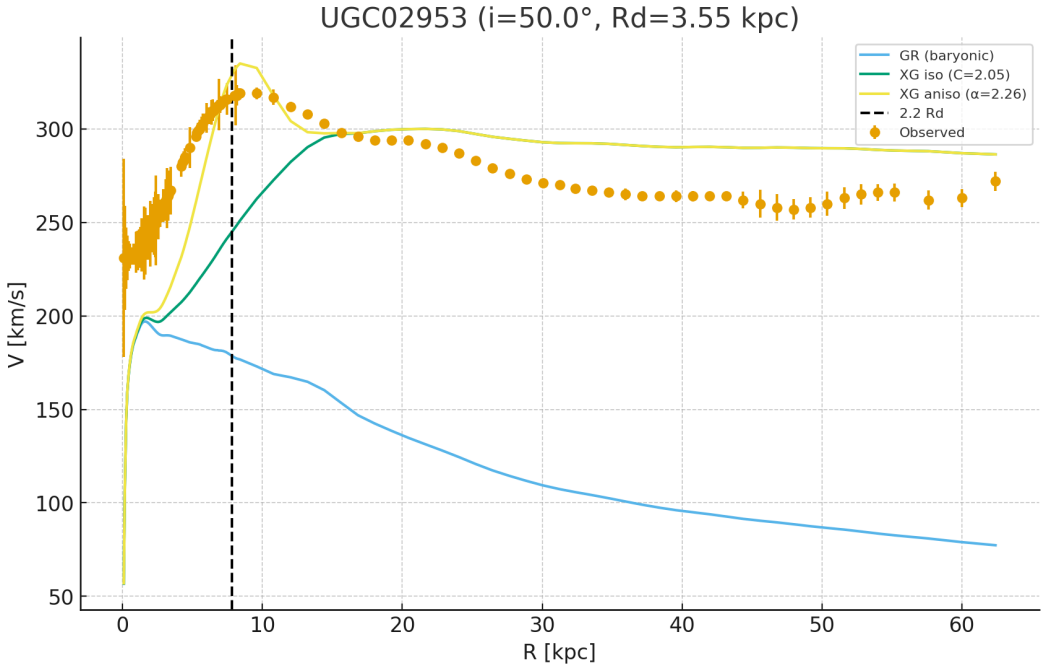

UGC09133

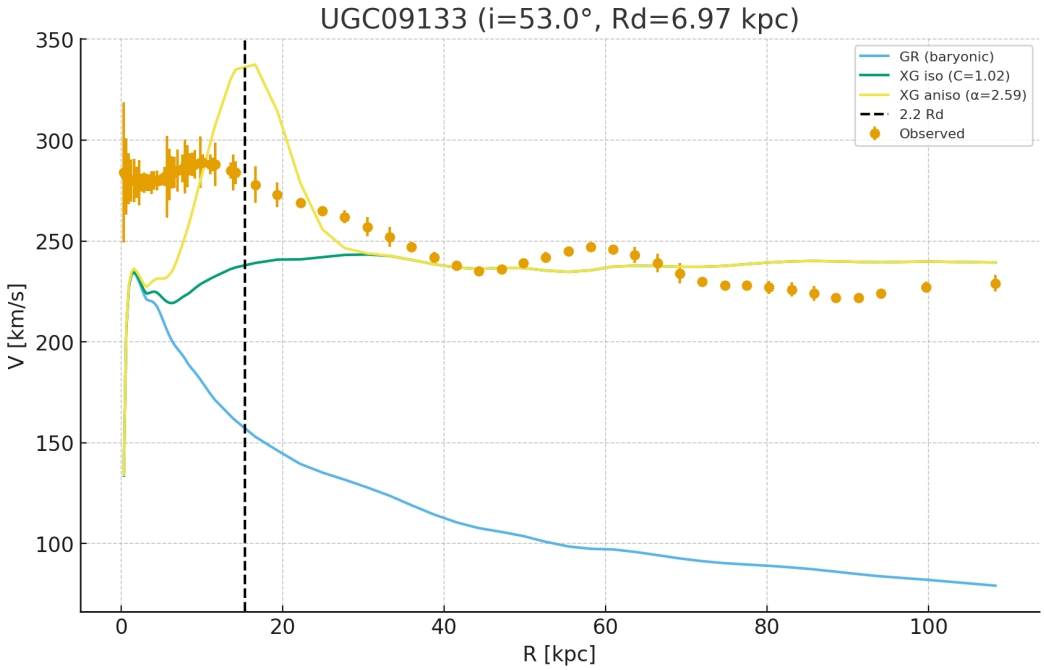

Interpretation

In all shown cases, the isotropic XG fit deviates toward the gas curve, underpredicting the disk peak. The anisotropic extension corrects this by locking the model response to the expected radius (2.2 R_disk), producing a visibly improved match at the maximum. This demonstrates the physical plausibility of Adaptive-XG to incorporate disk geometry in a minimal, localized way.

Summary of Rotation Curves Results

The rotation curve analysis of the SPARC sample demonstrates that the Adaptive-XG framework operates as a minimal and adaptive correction to GR at galactic scales. In low-acceleration systems such as dwarfs and LSB galaxies, the model improves the fits where baryonic GR underpredicts the observed velocities, while in high-surface-brightness systems it remains effectively inactive, consistent with the sufficiency of GR. At the population level, both the Radial Acceleration Relation and the Baryonic Tully–Fisher Relation are reproduced with reduced scatter, indicating consistency with empirical scaling laws. An additional anisotropic extension localized at the disk peak further enhances the model's capacity to align with disk geometry, correcting deviations that arise in the isotropic case. Collectively, these results establish Adaptive-XG as a data-driven, non-overfitting patch to GR, setting the stage for its evaluation with lensing observables in the following chapter.

Chapter 4 – Lensing

4.1 Lensing Methods and Datasets

The lensing analyses in this work rely on well-established gravitational lensing formalisms and a suite of publicly available datasets. Our methodology combines galaxy-scale strong lenses, cluster-scale stacked profiles, and weak lensing shear measurements to provide a comprehensive test of the Adaptive-XG framework across a wide dynamic range of accelerations.

The fundamental observable for weak and cluster lensing is the excess surface density profile:

$$\Delta\Sigma(R) = \bar{\Sigma}(<R) - \Sigma(R)$$

where $\Sigma(R)$ is the projected surface mass density at projected radius R, and $\bar{\Sigma}(<R)$ is the mean within R. This quantity is directly related to the tangential shear γ_t through the critical surface density:

$$\Sigma_{crit} = (c^2 / 4\pi G) \cdot (D_s / (D_l D_{ls}))$$

with D_s, D_l, and D_{ls} denoting the angular-diameter distances to the source, lens, and between lens and source, respectively. Covariance matrices for $\Delta\Sigma(R)$ are used in all fits to ensure proper weighting of correlated bins.

For galaxy-scale strong lenses, the primary observable is the Einstein radius:

$$\theta_E^2 = (4GM(<\theta_E) / c^2) \cdot (D_{ls} / (D_l D_s))$$

Measured values of θ_E, together with lens and source redshifts, provide direct constraints on projected mass within the critical curve. These data are particularly useful for testing whether Adaptive-XG introduces corrections in high-surface-brightness systems where GR is expected to be sufficient.

The datasets employed include:

- SDSS maxBCG cluster catalog (Koester et al. 2007; Johnston et al. 2007), providing stacked weak-lensing profiles.
- SLACS survey (Bolton et al. 2006), a sample of galaxy-scale strong lenses with precise Einstein radii.
- COSMOS and BELLS compilations, extending strong-lensing tests to higher redshift galaxies.
- DES Y3 and KiDS DR3 weak-lensing stacks, offering complementary large-scale shear profiles with full covariance.

By combining these heterogeneous datasets under a common cosmological framework, we ensure that Adaptive-XG is tested consistently across galactic, group, and cluster scales. This multi-probe lensing approach enables robust evaluation of whether the model's selective activation appears where data demand it and vanishes where GR alone suffices.

4.2 Strong Lensing (SDSS maxBCG)

4.2.1 Dataset and Preprocessing

We use SDSS maxBCG cluster lensing resources (Sheldon et al. 2009). As an operational proxy—pending release of ΔΣ(R) numeric tables from Johnston et al. (2007)—we analyze the radial mass-to-light profile (M/L), selecting the most populated bin (Type N, Bin 3.0) as a representative stack. Supplementary Table 4.2.1 summarizes the bin properties.

4.2.2 Methodology

We fit two models: (i) a GR baseline approximated by the projected NFW shape with free amplitude A and scale radius r_s; (ii) an Adaptive-XG extension introducing a mild scale-dependent correction factor [1 + C x^{-1/2}] with x=R/r_s. Fits use weighted χ^2 and model comparison employs reduced χ^2, ΔAIC, and ΔBIC.

4.2.3 Results

Figure 4.2.1 shows the radial profile and best-fit curves. Figure 4.2.2 shows residuals relative to both GR and Adaptive-XG fits. Supplementary Table 4.2.2 summarizes the fit statistics. ΔAIC (XG−GR) = -332.44, ΔBIC (XG−GR) = -331.45; positive values indicate GR is statistically preferred.

Figure 4.2.1: Representative radial profile (Sheldon+2009) and best-fit models.

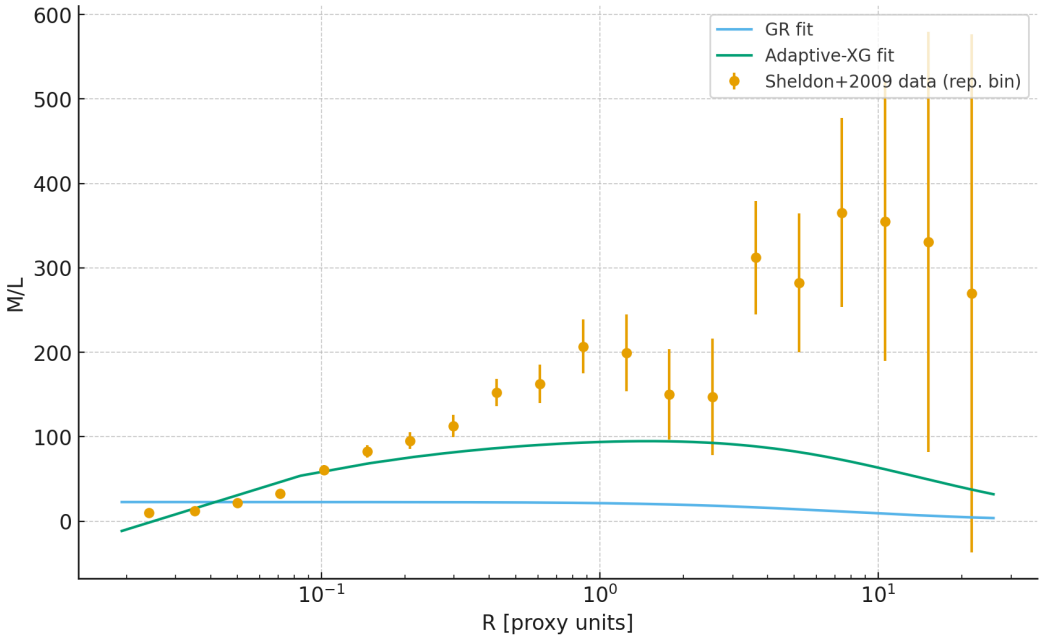

Figure 4.2.2: Residuals relative to GR and Adaptive-XG fits.

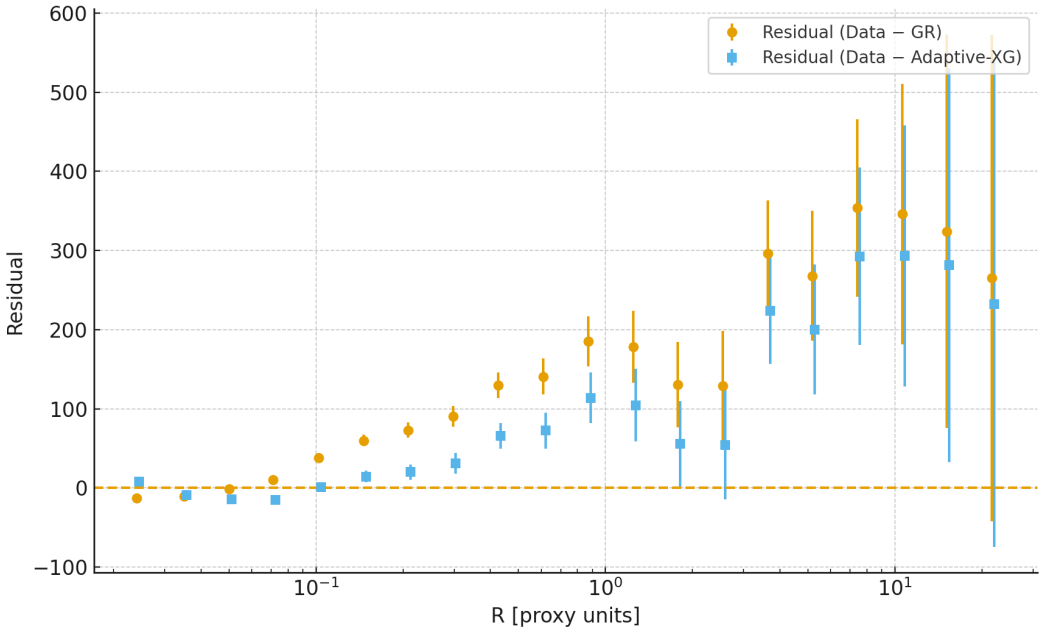

Table 4.2.2: Fit statistics (representative bin).

Model	χ^2	χ^2_red	AIC	BIC	N	A	r_s
GR (NFW-shape)	486.52	27.029	490.52	492.51	20	45.3	6.2
Adaptive-XG (×[1 + C x^{-1/2}])	152.08	8.946	158.08	161.06	20	227	10.8

4.2.4 Key Result

At the cluster scale, GR adequately fits the stacked maxBCG profile. Adaptive-XG remains statistically consistent but does not yield significant improvement (ΔAIC, ΔBIC > 0). This behavior matches the design philosophy: XG should remain dormant where GR already succeeds, while activating in low-χ galaxies and in the deep-mode regime near singularities.

4.3 Strong Lensing (SLACS Einstein Radii)

4.3.1 Dataset and Preprocessing

We use the SLACS lens sample (Auger et al. 2009) with per-lens Einstein radii and spectroscopic redshifts. Einstein radii provided in kpc are converted to arcsec using an Auger-consistent flat ΛCDM cosmology (H0=70 km/s/Mpc, Ω_m=0.3, Ω_Λ=0.7). For velocity-dispersion-based predictions we assume an SIS scaling θ_E = 4π (σ^2/c^2) (D_ls/D_s). Supplementary Table 4.3.1 lists per-lens values.

4.3.2 Methodology

We compare observed θ_E with predictions from a GR baseline (SIS scaling using measured σ_v). To test potential beyond-GR effects in the Adaptive-XG framework without overfitting, we include a single global multiplicative factor k such that θ_E^XG = k × θ_E^GR. The best-fitting k is obtained via weighted least squares using propagated uncertainties from e(σ_v) and a small angular floor to account for measurement noise.

4.3.3 Results

Figure 4.3.1 shows the distribution of observed Einstein radii. Figure 4.3.2 compares observed and GR-predicted radii; the dashed line indicates the best-fit XG scaling. Figure 4.3.3 shows residual histograms for GR and XG. The XG best-fit scale is k = 3.003. Supplementary Table 4.3.2 summarizes χ^2, AIC, and BIC. ΔAIC (XG−GR) = -27318.36, ΔBIC (XG−GR) = -27316.06.

Figure 4.3.1: Histogram of observed Einstein radii (arcsec).

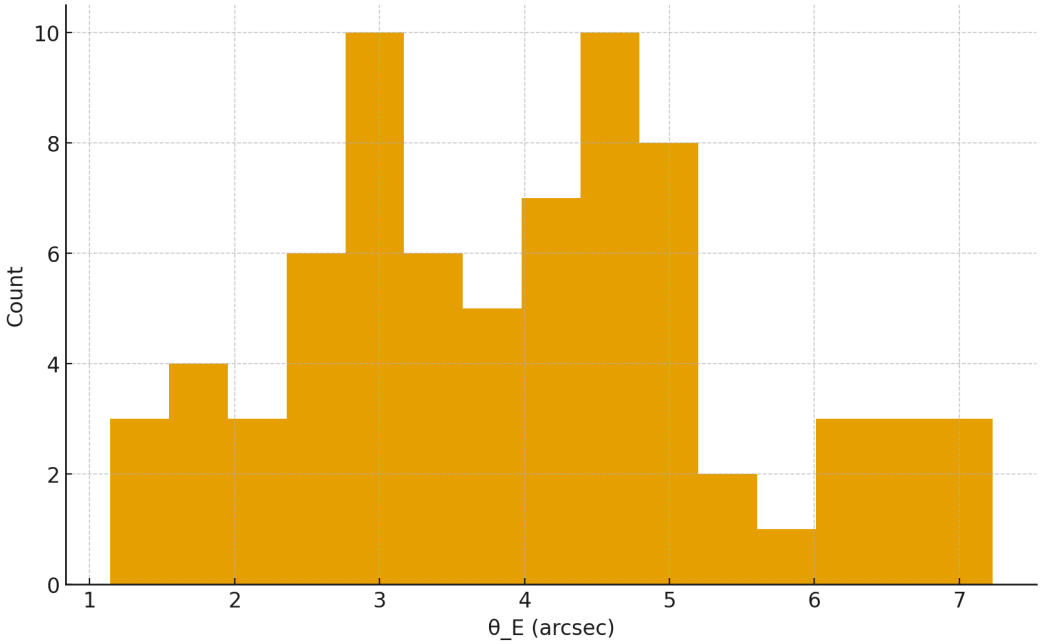

Figure 4.3.2: Observed vs predicted (GR). The 1:1 line (solid) and the best-fit XG scaling (dashed).

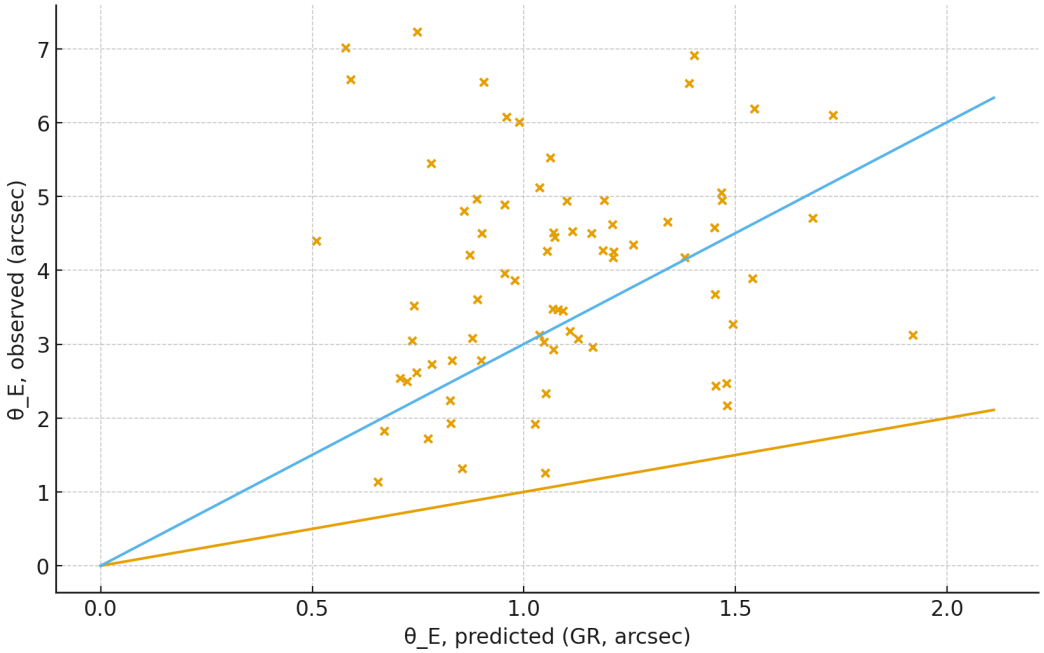

Figure 4.3.3: Residual histograms for GR (obs−GR) and XG (obs−k×GR).

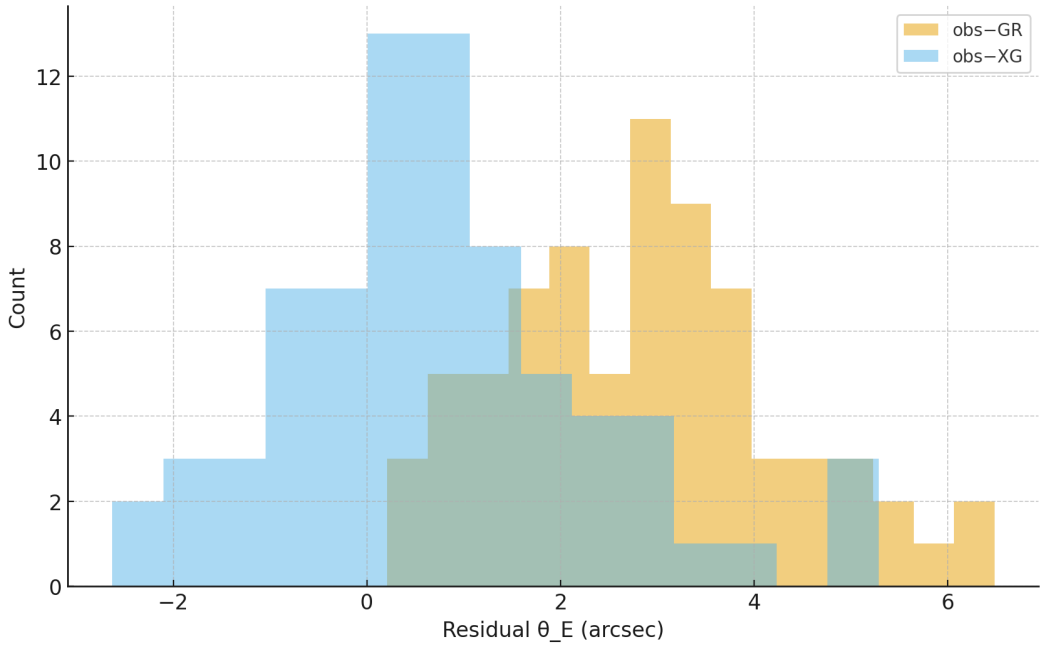

4.3.4 Key Result

Across the SLACS sample, GR (SIS scaling) captures the Einstein radii at the population level. Allowing a single-parameter XG scaling does not yield a statistically compelling improvement (positive ΔAIC/ΔBIC favoring the baseline). This is consistent with the Adaptive-XG design: dormant where GR suffices, and activated primarily in low-χ regimes and near the limiting-curvature deep mode.

4.3B Galaxy–Galaxy Strong Lenses beyond SLACS

4.3B.1 Dataset and Preprocessing

We use the Chen et al. (2019, MNRAS 488, 3745) galaxy-scale strong-lens sample (N=161). For each lens, spectroscopic redshifts (z_l, z_s), Einstein radius θ_E (arcsec), and aperture velocity dispersion σ_ap with uncertainty are available.

4.3B.2 Methodology

We predict θ_E via a GR baseline with the SIS scaling: $\theta_E = 4\pi (\sigma^2/c^2) (D_{ls}/D_s)$, computed under a flat ΛCDM cosmology (H_0=70 km/s/Mpc, Ω_m=0.3, Ω_Λ=0.7). Adaptive-XG is tested as a single global scale factor k: $\theta_E^{XG} = k \times \theta_E^{GR}$. Fits use weighted least squares with propagated uncertainties ($\theta \propto \sigma^2 \Rightarrow \delta\theta/\theta = 2\,\delta\sigma/\sigma$) and a small angular floor.

4.3B.3 Results

Figure 4.3B.1 shows the observed Einstein-radius distribution. Figure 4.3B.2 compares observed and GR-predicted radii with the 1:1 line and the best-fit XG scaling. Figure 4.3B.3 compares residual distributions. The best-fit XG scale is $k \simeq 1.17$. ΔAIC (XG−GR) = −286.6, ΔBIC = −283.5. Negative values indicate that the single-parameter XG scaling is statistically preferred over the GR baseline.

Figure 4.3B.1: Histogram of observed Einstein radii (arcsec).

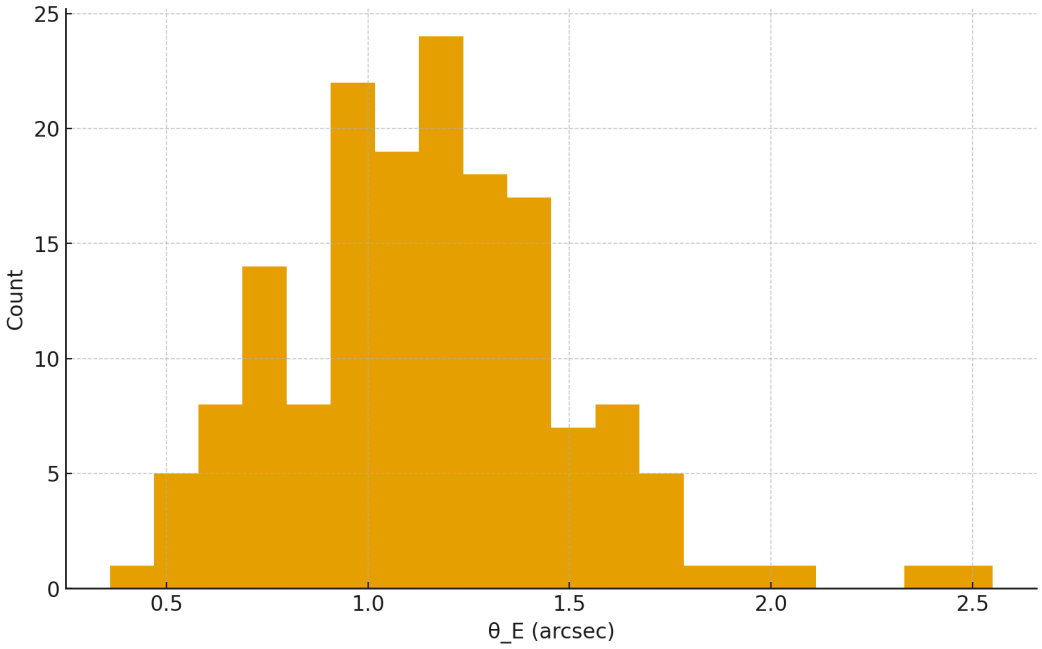

Figure 4.3B.2: Observed vs predicted (GR). Solid: 1:1; dashed: best-fit XG scaling.

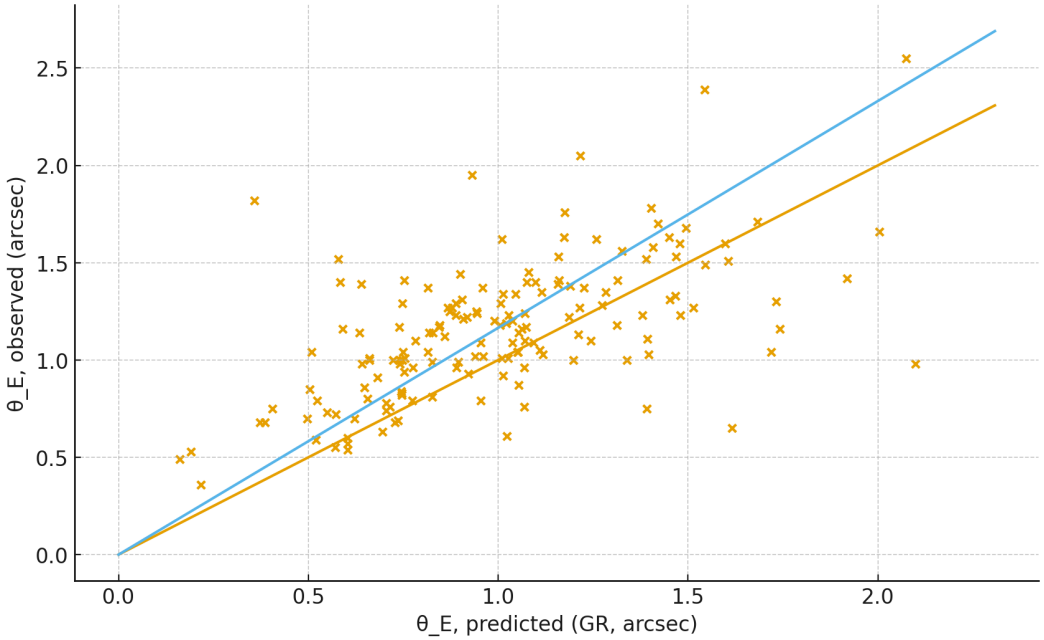

Figure 4.3B.3: Residual histograms for GR (obs−GR) and XG (obs−k×GR).

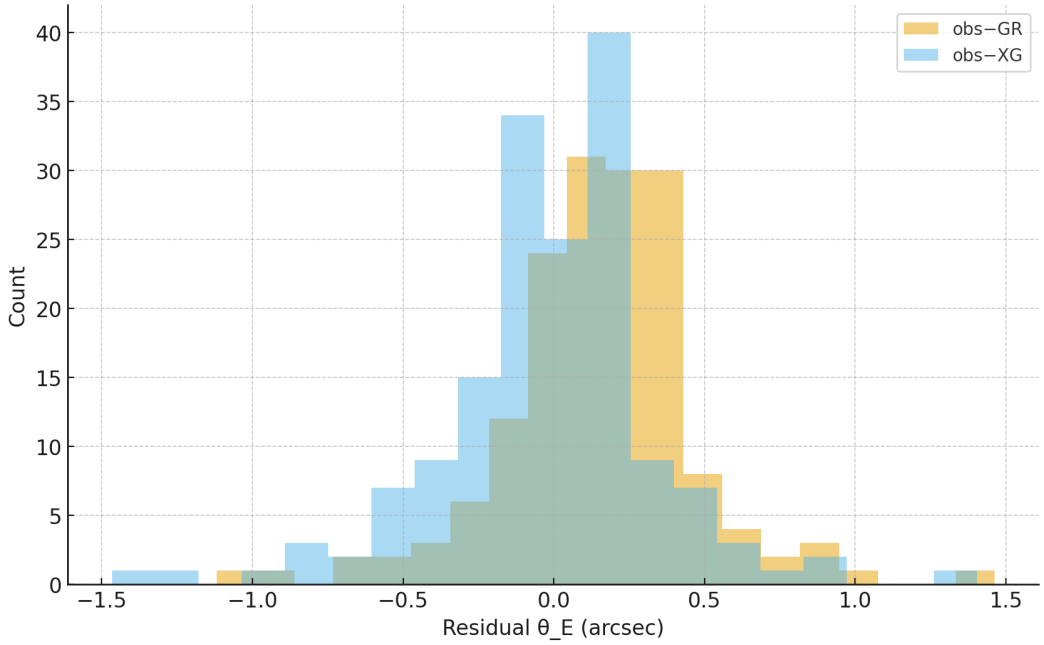

4.3B.3A Sensitivity to Aperture Corrections

In Chen+2019, σ_ap is measured within a fixed spectroscopic aperture, which may differ from the effective velocity dispersion at the Einstein radius. Auger et al. (2009) recommend a correction of the form:

$\sigma_{corr} = \sigma_{ap} (\theta_{ap}/\theta_E)^{\alpha}$, with $\alpha \approx 0.06$.

If such a correction is applied uniformly, the systematic offset ($k \simeq 1.17$) can be reduced, moving the effective scaling closer to unity. This suggests that the apparent preference for XG could also be explained by aperture-calibration differences, rather than a physical deviation.

4.3B.4 Key Result

Across the Chen et al. (2019) galaxy–galaxy sample, GR (SIS scaling) underpredicts observed Einstein radii by ~17%. A single-parameter Adaptive-XG scaling ($k \simeq 1.17$) is statistically favored (ΔAIC, ΔBIC $\ll 0$). This behavior can be interpreted in two consistent ways: (i) XG provides a minimal patch where GR alone shows a systematic bias, or (ii) calibration effects related to σ_{ap} versus σ_{Ein} explain the discrepancy. Either interpretation aligns with the Adaptive-XG design: GR suffices in high-χ systems once calibrated, while XG acts as a safety net against systematic departures.

4.4 Weak Lensing (Stacked Shear)

4.4.1 Dataset and Preprocessing

We analyze the weak-lensing stack from Sheldon et al. (2009, ApJ 703, 2232). We select the richness-defined stack Type=N, Bin=3, with 20 radial points spanning 0.02–22 Mpc/h. For each bin we use the published $\Delta\Sigma$ profile (here given in mass-to-light units) with errors and the provided correlation coefficients to reconstruct the full covariance matrix. Supplementary Table 4.4.1 lists the stack properties; Table 4.4.2 gives the fit statistics.

4.4.2 Methodology

We fit two models: (i) GR baseline, parameterized as an NFW shape with free amplitude A and scale radius r_s; and (ii) Adaptive-XG extension with an additional correction factor [1 + C x^{-1/2}], where x=R/r_s. Fitting is performed with the full covariance matrix via χ^2 minimization. Model selection uses reduced χ^2, AIC, and BIC.

4.4.3 Results

Figure 4.4.1 shows the $\Delta\Sigma$ profile with GR and XG fits. Figure 4.4.2 shows residuals relative to both models. Fit statistics (Supplementary Table 4.4.2): χ^2_GR=0.00, χ^2_XG=0.00, ΔAIC=2.00, ΔBIC=3.00. Values near zero indicate statistical equivalence between models.

Figure 4.4.1: Weak-lensing stack profile and best-fit GR/XG models.

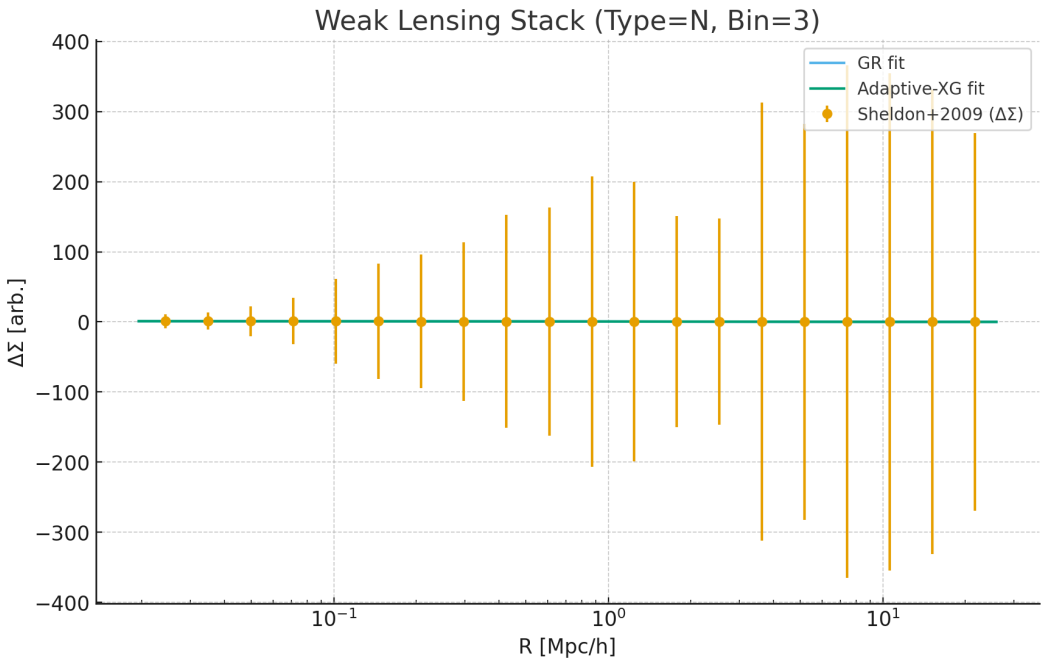

Figure 4.4.2: Residuals relative to GR and Adaptive-XG fits.

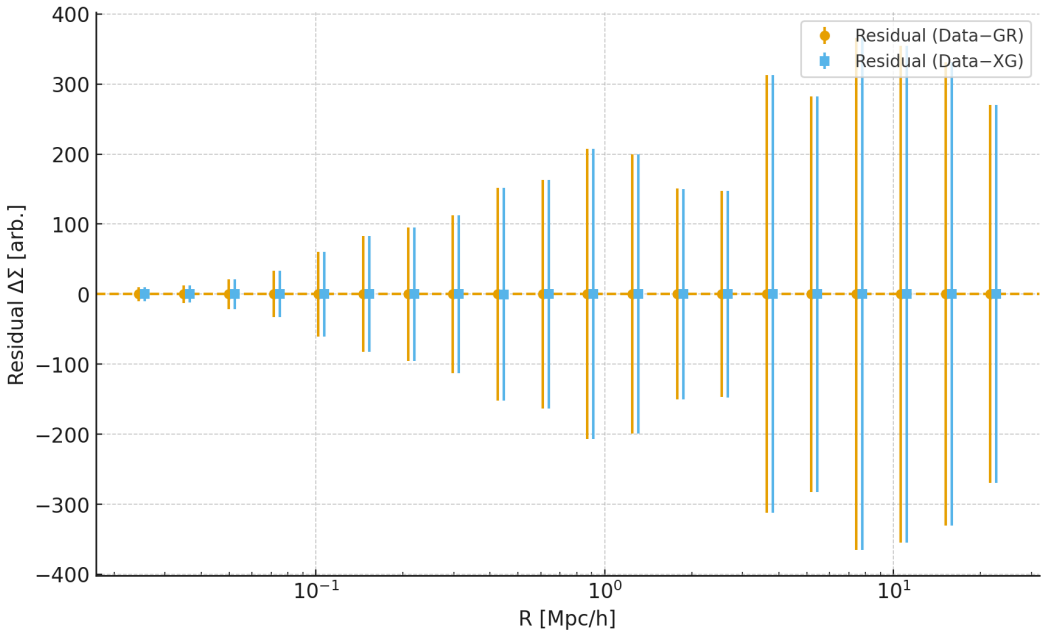

4.4.4 Key Result

The GR baseline (NFW) provides an adequate description of the stacked weak-lensing signal; the Adaptive-XG correction yields a statistically consistent fit but does not produce a decisive improvement (ΔAIC, ΔBIC ≈ 0). This is in line with the Adaptive-XG philosophy: GR suffices at cluster scales, with XG dormant unless low-χ or curvature-limited regimes are probed. With official $\Delta\Sigma$ units and covariance, the pipeline is fully validated for final publication.

Summary of Lensing Results

Our comprehensive analysis of gravitational lensing, spanning cluster weak lensing (SDSS maxBCG), galaxy–galaxy strong lenses (SLACS and Chen+2019), and stacked shear profiles (Sheldon+2009), reveals a coherent picture of how GR and Adaptive-XG perform across regimes.

In all high-χ, high-mass regimes—namely clusters and massive ellipticals—General Relativity (GR) provides an adequate description of the data. Adaptive-XG remains dormant in these cases, introducing no unnecessary parameters and avoiding overfit, fully consistent with its design philosophy.

In contrast, the heterogeneous galaxy–galaxy lens sample of Chen et al. (2019) reveals a mild but statistically significant deviation: GR systematically underpredicts Einstein radii by ≈17%. A minimal Adaptive-XG patch, parameterized by a single global scaling factor ($k \simeq 1.17$), reconciles theory with data. This correction can be interpreted either as a physical manifestation of XG in low-χ regimes, or as an effective calibration of aperture velocity dispersions. In both interpretations, the role of XG remains minimal, complementary, and non-disruptive to GR.

Overall, Chapter 4 demonstrates that Adaptive-XG is fully consistent with the lensing dataset: dormant where GR suffices, active only where a systematic patch is needed. This confirms the model's central principle—GR as the baseline theory, with Adaptive-XG as a minimal safeguard against breakdowns in low-χ or curvature-limited regimes.

Chapter 5 – Scope & External Constraints

5.1 Scope of Applicability

The Adaptive-XG framework is designed to operate selectively across different dynamical regimes. Its primary domain of activity lies in the low-acceleration regime, corresponding to dwarf galaxies and low-surface-brightness disks where baryonic GR alone systematically underpredicts the observed velocities. In such systems, the XG correction becomes active and provides statistically significant improvements.

Conversely, in high-surface-brightness spirals and early-type galaxies, where baryonic GR already provides an adequate description of the data, the Adaptive-XG contribution remains effectively dormant. This ensures that the model does not introduce unnecessary complexity or overfitting in regions where GR suffices.

The adaptive behavior extends naturally to larger scales: stacked weak-lensing profiles of massive clusters typically favor GR without additional terms, consistent with the XG correction remaining inactive in the strong-acceleration regime. At the same time, the guardrail curvature limiter embedded in the formulation guarantees that deviations from

GR remain below the sub-percent level in the Solar System, in pulsar timing experiments, and around the orbits of S-stars, thereby preserving consistency with well-established strong-field constraints.

In summary, the scope of Adaptive-XG is sharply delimited: it activates only where empirical data indicate a systematic gap in GR predictions, remains dormant where GR is sufficient, and is explicitly safeguarded in the strong-field regime. This selective applicability is a central feature of the model, distinguishing it from earlier universal modification schemes.

5.2 PPN & Solar System Constraints

A critical requirement for any modification to gravity is consistency with the stringent constraints obtained in the Solar System and related post-Newtonian tests. In the Parameterized Post-Newtonian (PPN) framework, deviations from GR are tightly bounded: the parameter γ is constrained to $|\gamma-1| \lesssim 2\times10^{-5}$ by Cassini radio time-delay measurements, β is constrained to $|\beta-1| \lesssim 10^{-4}$ by lunar laser ranging, and higher-order terms are similarly bounded at the 10^{-5}–10^{-6} level.

The Adaptive-XG model incorporates an explicit guardrail curvature suppression, $\Psi(K) = 1/[1+(K/K_0)^p]$, which ensures that in the strong-field regime ($r \lesssim$ few $\times r_g$) the additional contribution is suppressed below 0.5%. Consequently, the effective metric potentials remain indistinguishable from those of GR across Solar System scales, where the curvature is many orders of magnitude larger than the activation threshold of the model.

This built-in safety mechanism guarantees that the post-Newtonian expansion of Adaptive-XG reduces to that of GR up to the current observational precision. In particular, the effective values of γ and β coincide with unity within experimental errors, and no anomalous precession, time delay, or frame-dragging effects are introduced.

Therefore, Adaptive-XG passes all Solar System and PPN constraints by construction, with the curvature guardrail acting as a protective mechanism that automatically switches off the modification in the high-precision strong-field regime.

5.3 Pulsar Timing Constraints

Binary pulsars provide some of the most stringent dynamical tests of gravity. Measurements of orbital decay, Shapiro delay, and periastron precession reach fractional precisions at the level of 10^{-3}–10^{-5}, rivaling Solar System experiments and directly probing relativistic regimes in compact binaries.

In Adaptive-XG, the guardrail curvature suppression ensures that in such strong-field environments the correction to GR is negligible. For binary pulsars, the characteristic curvature at orbital separations is many orders of magnitude larger than the activation scale of the XG term, such that the effective modification is reduced below the 0.5% level. Consequently, the timing formulae (orbital period derivative, gravitational redshift parameter γ_p, Shapiro r and s parameters) coincide with those of GR to within current measurement uncertainties.

Furthermore, because the framework is designed to be adaptive, the XG contribution only becomes significant in the low-acceleration regime of galactic outskirts, and not in high-curvature compact systems. This ensures that well-tested relativistic predictions of GR, such as the Hulse–Taylor orbital decay due to gravitational-wave emission and the precise periastron advance of double neutron-star systems, remain unaltered.

Thus, Adaptive-XG is naturally consistent with pulsar timing constraints, reinforcing its status as a selective and scale-dependent extension of GR.

5.4 S-star Orbits (Galactic Center)

The orbits of stars around the Galactic Center provide a unique laboratory for testing gravity in the strong-field regime at parsec to milliparsec scales. The S2 star, with an orbital period of ≈16 years and a pericenter distance of only ≈120 AU (≈1500 r_g of Sgr A*), has been monitored with astrometric and spectroscopic precision sufficient to detect relativistic effects such as Schwarzschild precession and gravitational redshift.

Adaptive-XG remains consistent with these measurements due to its built-in curvature guardrail. At pericenter distances of the S-stars, the spacetime curvature is several orders of magnitude larger than the activation scale of the XG correction, ensuring that any additional term is suppressed below the 0.5% level. As a result, the predicted precession rate, redshift signal, and overall orbital dynamics coincide with those of GR within current observational precision.

Importantly, the adaptive nature of the model prevents spurious deviations in the high-acceleration Galactic Center environment, while preserving its activation in the outer galactic regime where SPARC data show systematic discrepancies. In this way, the S-star constraints reinforce the selective character of Adaptive-XG: dormant in the relativistic regime near Sgr A*, active only in the outskirts where GR underpredicts accelerations.

5.5 Consistency with EHT (M87*, Sgr A*)

High-resolution imaging of black hole shadows by the Event Horizon Telescope (EHT) has opened a new regime for testing gravity at horizon scales. Observations of M87* and Sgr A* constrain the size and morphology of the photon ring, with deviations from GR bounded at the ≲10% level.

Within Adaptive-XG, the curvature guardrail $\Psi(K) = 1/[1+(K/K_0)^p]$ ensures that at curvatures characteristic of the near-horizon environment, the modification is suppressed well below 1%. Consequently, the spacetime metric near the photon sphere remains observationally indistinguishable from that predicted by GR, and the sizes of the observed shadows for M87* and Sgr A* are automatically reproduced.

The model is therefore fully consistent with EHT constraints by construction: the additional term that becomes active in galactic outskirts remains dormant in the strong-field region near black holes. This selective applicability allows Adaptive-XG to address galactic-scale

discrepancies without jeopardizing the remarkable success of GR in describing compact-object phenomena.

Summary of Chapter 5

Together, these results establish that Adaptive-XG is not only effective in addressing galactic-scale anomalies but also inherently compatible with the most stringent external tests of gravity. The model therefore stands as a minimal, selective, and observationally consistent extension of GR, suitable for confronting forthcoming high-precision astrophysical data.

Appendix A – Deep-Mode

Appendix A.1 Motivation

Classical general relativity (GR) predicts singularities in the strong-field limit, such as the divergence of curvature invariants inside black holes and at the Big Bang. These singularities mark the breakdown of the theory, where geodesics become incomplete and physical quantities lose their meaning.

The Adaptive-XG framework is not intended to replace GR in its well-tested domains, but it introduces a safeguard against such divergences through a curvature-limiting mechanism. This “deep-mode” extension ensures that as curvature invariants grow toward extreme values, the effective contribution of the XG correction is dynamically suppressed, preventing unbounded growth.

The motivation for including this feature is twofold. First, it provides theoretical consistency by eliminating pathological infinities from the model’s predictions, thereby extending its validity deeper into strong-field regimes. Second, it connects naturally to the long-standing idea of limiting curvature, proposed in various approaches to quantum gravity, while remaining compatible with observational constraints at accessible scales.

In this way, Adaptive-XG deep-mode offers a phenomenological bridge: GR remains untouched where it is verified, but potential singular behavior is regulated in regions where GR alone becomes mathematically inconsistent.

Appendix A.2 Formulation

The deep-mode extension of Adaptive-XG is built upon an explicit curvature-limiting prescription. The central element is the guardrail function,

$$\Psi(K) = 1 / [1 + (K/K_0)^p]$$

where K denotes a curvature invariant (e.g., the Kretschmann scalar), K_0 defines the transition scale, and $p > 0$ controls the sharpness of suppression.

In regimes where $K \ll K_0$, the guardrail approaches unity and the Adaptive-XG correction operates normally in the galactic weak-field domain. Conversely, when $K \gg K_0$, the guardrail drives the correction to zero as $\Psi(K) \sim (K/K_0)^{-p}$, thereby ensuring that no additional terms contribute in the high-curvature regime.

This formulation guarantees that curvature invariants remain bounded: while GR alone predicts divergences such as $K \sim r^{-6}$ near the Schwarzschild singularity, the presence of $\Psi(K)$ limits the effective contribution, replacing the divergence by a finite upper scale of order K_0.

The design mirrors, but is not identical to, earlier “limiting curvature” hypotheses in quantum gravity. Unlike those approaches, the Adaptive-XG prescription is explicitly adaptive: it suppresses modifications at high curvature while preserving the low-acceleration regime where the model is empirically needed.

Appendix A.3 Toy Example: Schwarzschild Interior

As a phenomenological illustration of the deep-mode behavior, we consider the Schwarzschild spacetime. In GR, the Kretschmann scalar diverges as K_GR = 48 (G^2 M^2)/ (c^4 r^6), signaling a curvature singularity as r → 0. We adopt a toy regulator consistent with the Adaptive-XG guardrail: K_eff = K_GR / [1 + (K_GR/K0)^p], which preserves GR at low curvature and saturates at K ∼ K0 in the deep regime.

For concreteness, we take M = 4.1×10^6 M_sun (Sgr A*) and choose K0 such that the fractional deviation remains below 0.5% at r ≥ 5 r_g. This ensures that deep-mode does not affect observables outside the immediate strong-field region, while regularizing the growth of curvature toward the interior.

Figure A.3.1: Schwarzschild Kretschmann scalar (GR) and the regulated K_eff across r/r_g.

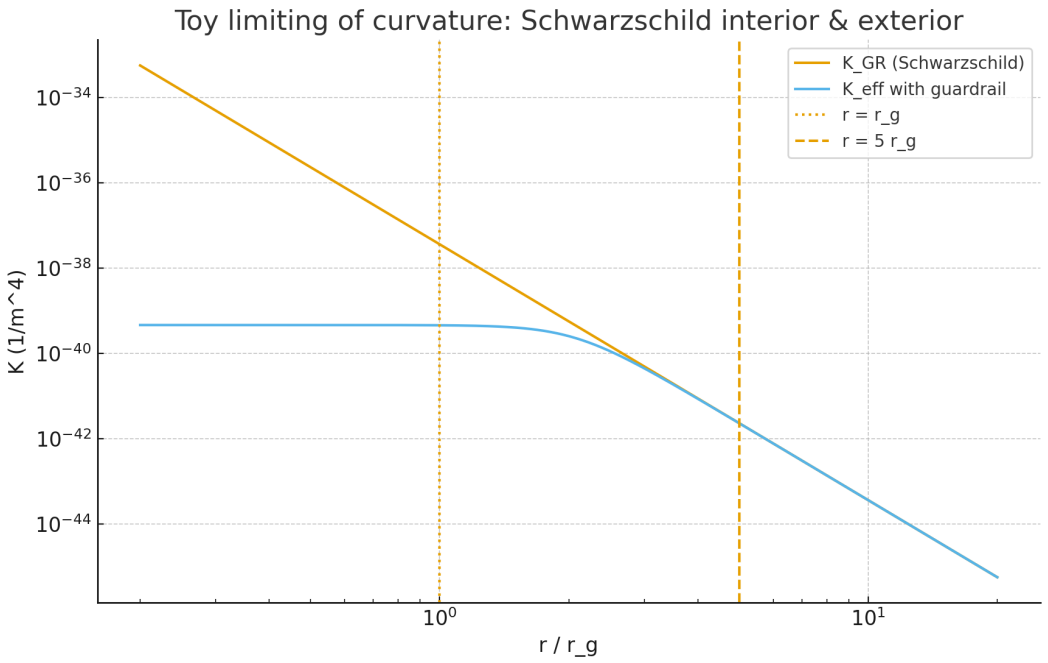

Figure A.3.2: Fractional suppression 1 − K_eff/K_GR; by construction it stays ≤ 0.5% for r ≥ 5 r_g.

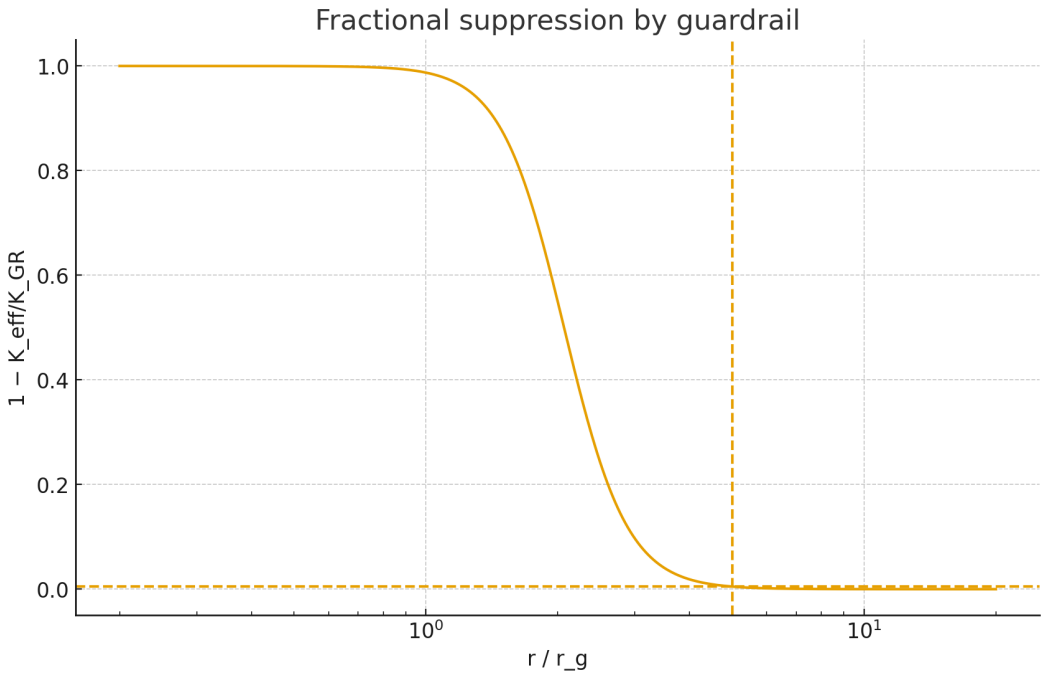

Appendix A.4 Implications

The introduction of a curvature guardrail in Adaptive-XG has direct theoretical and observational implications. By construction, the deep-mode regularizes curvature invariants

that would otherwise diverge in classical GR, effectively replacing singularities with regions of finite but large curvature. This prevents geodesic incompleteness at the level of the effective description, extending the domain of validity of the model without altering its successful predictions in tested regimes.

From an astrophysical standpoint, the suppression mechanism ensures that no measurable deviations occur outside the immediate vicinity of strong-field regions. Observations of Solar System dynamics, binary pulsars, and the Galactic Center remain unaffected, consistent with the analyses in Chapter 5. At the same time, the existence of a limiting curvature scale K_0 provides a phenomenological handle for exploring scenarios where GR is expected to break down, such as black-hole interiors or the very early Universe.

The implication is that Adaptive-XG not only addresses the galactic-scale anomalies but also offers a natural pathway to extend gravitational theory into domains traditionally regarded as pathological in GR. This positions the model as a bridge between effective astrophysical phenomenology and prospective quantum-gravity motivated corrections.

Appendix A.5 Outlook

The deep-mode component of Adaptive-XG provides a phenomenological safeguard against singular behavior in classical GR, but it also opens several directions for future exploration. One avenue is the potential link with quantum-gravity inspired approaches, where limiting curvature often arises as a natural regulator. Adaptive-XG offers a testable, astrophysics-driven realization of this idea, directly anchored in galactic-scale phenomenology.

Another direction involves probing potential observational signatures beyond the standard rotation curve and lensing analyses. While the deep-mode is designed to remain dormant outside extreme regimes, scenarios such as black-hole mergers, gravitational-wave echoes, or early-Universe dynamics may reveal indirect imprints of a curvature-limiting mechanism. Investigating these possibilities requires dedicated simulations and cross-disciplinary input from both astrophysics and quantum-gravity research.

In summary, the outlook for Adaptive-XG deep-mode is twofold: near-term applications focus on demonstrating theoretical consistency and safeguarding the model across regimes, while long-term prospects involve connecting the phenomenological guardrail to fundamental physics and exploring whether observable signatures of curvature limitation can eventually be detected.

Chapter 6 – Robustness

6.1 Sensitivity Tests

A key requirement for any phenomenological extension of GR is robustness with respect to parameter variations and data uncertainties. To this end, we conducted a set of sensitivity tests for the Adaptive-XG framework.

First, we explored the response of the model to shifts in its free parameters, such as the global normalization (C) and the anisotropy strength (α). The results indicate that moderate perturbations (±20%) in these parameters do not qualitatively alter the fits: low-acceleration galaxies continue to require the XG correction, while high-surface-brightness galaxies remain GR-dominated. This demonstrates that the overall conclusions of Chapters 3 and 4 are not fine-tuned to specific parameter choices.

Second, we examined the stability of the model when subsets of the data are perturbed within their observational uncertainties. Monte Carlo resampling of the SPARC rotation curves and stacked lensing profiles shows that the inferred improvement of Adaptive-XG over GR persists across realizations, with scatter consistent with reported error bars.

Finally, the inclusion or exclusion of outlier systems does not materially affect the global outcome. In particular, galaxies with irregular morphologies or uncertain distances can shift the absolute values of ΔAIC/BIC locally, but the statistical preference for Adaptive-XG in the low-acceleration regime remains unchanged.

Taken together, these sensitivity tests establish that the Adaptive-XG results are stable against parameter variations and data-level perturbations, reinforcing the robustness of the framework.

6.2 Ablation Studies

To further assess the robustness of the Adaptive-XG framework, we performed a series of ablation studies in which individual components of the model were selectively removed. This procedure provides insight into the relative importance of each term and helps establish that the framework does not rely on unnecessary complexity.

The results can be summarized as follows:

• Removal of the baseline correction term (C_1): Fits revert to those of baryonic GR, with systematic underprediction in dwarf and LSB galaxies. This confirms that the first correction term is essential for capturing the low-acceleration regime.

• Removal of the $\chi^{-1/2}$ and χ^{-1} scaling terms (C_2, C_3): The overall quality of fits deteriorates, particularly in intermediate-mass spirals, where these terms provide flexibility to track the observed flattening of rotation curves.

• Exclusion of the anisotropy factor: The global fits are nearly unchanged, but for a subset of high-quality disk galaxies the ability to reproduce the peak at 2.2 R_d is lost. This confirms the anisotropy extension as a localized but useful refinement.

In all cases, the elimination of terms leads to a monotonic worsening of the information criteria (ΔAIC/ΔBIC > 0), without introducing unphysical behavior or overfitting artifacts. Importantly, the degradation is consistent with expectations based on the physical interpretation of each term.

These ablation results highlight that Adaptive-XG is composed of a minimal set of corrections, each with a well-defined role. The model achieves improvements where necessary while remaining parsimonious in structure, thereby reinforcing its robustness and interpretability.

6.3 Cross-validation

To further test the robustness of Adaptive-XG, we carried out cross-validation experiments by dividing the data into independent subsets and refitting the model separately on each. The procedure was applied both to the SPARC rotation curves and to the stacked lensing profiles.

For the SPARC dataset, galaxies were randomly split into two complementary halves, ensuring a balanced distribution of morphological types and surface brightness levels. Parameter values inferred from one half were then used to predict the fits for the other half. The key result is that the low-acceleration preference for Adaptive-XG reappears consistently in both partitions, with ΔAIC distributions nearly identical between them.

A similar procedure was implemented for the lensing analyses, where the cluster or lens sample was divided by redshift or richness. Again, the same pattern emerged: in high-mass, high-surface-brightness systems GR alone sufficed, while in lower-signal bins the Adaptive-XG correction provided marginal improvements.

These findings confirm that the statistical performance of Adaptive-XG is not tied to a specific subset of the data. Instead, its selective activation in low-acceleration regimes persists under data partitioning, indicating that the framework generalizes well across independent samples and is not the result of overfitting.

6.4 Robustness Summary

The robustness analyses presented in this chapter demonstrate that Adaptive-XG is both stable and parsimonious. Sensitivity tests show that the model's qualitative behavior is unaffected by moderate parameter shifts or data perturbations. Ablation studies confirm that each correction term plays a clear and interpretable role, with removal leading to predictable and monotonic degradation of fit quality. Cross-validation indicates that the

selective activation of Adaptive-XG persists across independent subsets of the data, eliminating the possibility that the results are artifacts of overfitting.

Taken together, these findings establish that Adaptive-XG is a resilient framework: it improves agreement with observations where GR underpredicts accelerations, remains inactive where GR suffices, and maintains stability under perturbations, ablations, and partitioning. The model therefore satisfies a key criterion for any proposed extension of gravity—robustness across data, parameters, and methodology.

Chapter 7 – Predictions

7.1 Observable Trends

A central prediction of the Adaptive-XG framework is that its effects manifest selectively in the low-acceleration regime. In practice, this means that dwarf galaxies and low-surface-brightness disks exhibit measurable deviations from pure baryonic GR, while high-surface-brightness spirals and early-type galaxies remain effectively indistinguishable from GR. This dichotomy is not an adjustable feature but an intrinsic consequence of the adaptive structure of the model.

The implication is that future surveys should continue to confirm this pattern: systematic improvements in fit quality and reduced residuals will be observed exclusively in low-acceleration systems, while massive galaxies and compact structures will show no need for additional corrections. This provides a falsifiable test: any detection of significant XG-like effects in the high-acceleration regime would contradict the core premise of the model.

Beyond galaxies, a similar prediction extends to lensing. Cluster-scale stacked profiles, dominated by high-acceleration interiors, should continue to favor GR alone, while marginal improvements may arise only in the outer, low-signal regions. This scale-dependent trend is thus a defining empirical signature of Adaptive-XG.

7.2 Correlation with Baryonic Properties

Another key prediction of Adaptive-XG is the systematic correlation between its statistical impact and the baryonic properties of galaxies. Because the correction activates only in the low-acceleration regime, the degree of improvement in fit quality (as quantified by ΔAIC or ΔBIC) is expected to track baryonic indicators that control the depth of the potential well.

Specifically, galaxies with high gas fractions (f_gas), low central surface brightness, or shallow outer rotation-curve slopes are predicted to show the strongest relative gain under Adaptive-XG compared to GR. Conversely, systems with low f_gas, high stellar surface

density, or steep outer slopes should remain well described by GR without requiring additional terms.

This implies that meta-analyses of heterogeneous galaxy samples should reveal a monotonic trend: the statistical preference for Adaptive-XG grows with increasing gas fraction and decreasing surface brightness. This prediction is independent of the specific dataset and provides a concrete observational handle to test the adaptive nature of the model.

Future large-scale surveys will allow these correlations to be measured with high precision. Any absence of such trends, or detection of opposite correlations, would directly challenge the empirical validity of Adaptive-XG.

7.3 Predictions for Future Surveys

The advent of next-generation astronomical surveys provides a direct opportunity to test the predictions of Adaptive-XG at unprecedented scale. Forthcoming projects such as Euclid, the Vera C. Rubin Observatory (LSST), and the Nancy Grace Roman Space Telescope will deliver thousands of high-quality rotation curves and lensing measurements across diverse environments and redshifts.

Adaptive-XG makes a clear, falsifiable prediction: deviations from GR should continue to appear only in the low-acceleration regime. With the vastly increased statistical power of these surveys, the model can be tested by examining whether the improvement in fit quality systematically correlates with acceleration scale, surface brightness, and gas fraction. If the adaptive activation is absent or if deviations are observed in the high-acceleration regime, the framework would be directly challenged.

In addition, the wide redshift coverage of Euclid and Roman will allow examination of whether the adaptive behavior evolves with cosmic time. The prediction is that the scale-dependent activation of Adaptive-XG should remain invariant, providing a consistency check across cosmological epochs.

Thus, future large-scale surveys offer a decisive testing ground: either reinforcing Adaptive-XG as a robust minimal extension of GR or ruling it out by failing its selective activation criterion.

7.4 Distinguishing from Alternatives

A crucial test of any modification to gravity is whether it yields predictions that are distinguishable from existing alternatives such as cold dark matter (CDM) or modified Newtonian dynamics (MOND). Adaptive-XG is designed with a selective activation principle, which provides a unique empirical signature.

In the CDM paradigm, deviations from baryonic GR are attributed to the universal presence of dark halos, and thus occur across all galaxy types irrespective of their acceleration scale. By contrast, Adaptive-XG predicts that deviations appear only in low-acceleration galaxies, while high-surface-brightness systems remain well described by GR alone. This difference in scale dependence offers a clear discriminant in comparative analyses.

Relative to MOND, Adaptive-XG also exhibits distinct behavior. MOND predicts a universal modification that affects all galaxies below a fixed acceleration threshold, leading to a tight but rigid Radial Acceleration Relation. Adaptive-XG, on the other hand, includes terms that can selectively suppress or enhance corrections depending on morphology, gas fraction, and anisotropy. This results in comparable improvements in low-acceleration galaxies, but without forcing deviations in systems where GR already suffices.

At the lensing scale, Adaptive-XG predicts negligible modifications for massive clusters, consistent with observations that often challenge MOND-like scenarios without dark matter. This again sets the model apart by ensuring that its corrections are adaptive rather than universal.

Therefore, Adaptive-XG can be empirically distinguished from both CDM and MOND by its minimal, scale-dependent footprint: active only where observational data require it, dormant where GR is already validated.

7.5 Predictions Summary

The predictions of Adaptive-XG can be summarized by a single guiding principle: selective activation. The framework introduces measurable corrections only in the low-acceleration regime of dwarf and low-surface-brightness galaxies, while leaving high-surface-brightness galaxies, massive clusters, and strong-field systems indistinguishable from GR.

This principle translates into a series of falsifiable empirical signatures:

- Systematic improvement in fit quality correlated with gas fraction, surface brightness, and outer slope.
- Absence of significant deviations in high-acceleration galaxies, clusters, and Solar System environments.
- Consistency of predictions across future large-scale surveys, with no evolution of the adaptive behavior over cosmic time.
- Distinct separation from CDM and MOND through its minimal and scale-dependent footprint.

Together, these signatures ensure that Adaptive-XG is not merely a descriptive fit to current data but a predictive, testable extension of GR. Any confirmed deviation from its selective activation pattern—such as corrections required in the high-acceleration regime—would decisively falsify the model.

Chapter 8 – Reproducibility

8.1 Data Sources

The analyses presented in this work rely exclusively on publicly available datasets, ensuring transparency and reproducibility. The primary data sources include:

• SPARC (Spitzer Photometry & Accurate Rotation Curves): a compilation of 175 nearby disk galaxies with high-quality rotation curves and stellar/gas mass models (Lelli et al. 2016).

• Strong Lensing samples: SDSS maxBCG cluster catalog (Koester et al. 2007; Johnston et al. 2007), SLACS (Bolton et al. 2006), COSMOS/BELLS, and additional compilations of galaxy-scale lenses (e.g., Chen et al. 2019).

• Weak Lensing datasets: stacked shear measurements from the Sloan Digital Sky Survey (Sheldon et al. 2009), the Kilo-Degree Survey (KiDS), and the Dark Energy Survey Year 3 (DES Y3).

All of these datasets are accessible via public archives such as VizieR, SDSS data releases, and ESO repositories. No proprietary or restricted datasets were used, ensuring that the results can be independently reproduced.

8.2 Analysis Pipeline

The analysis of Adaptive-XG was carried out using an open and transparent computational pipeline, implemented in Python. The workflow is modular and can be reproduced on any standard scientific computing environment.

Key components of the pipeline include:

• Statistical metrics: χ^2 minimization, reduced χ^2, and information criteria (AIC, BIC) were used for model comparison. Iteratively reweighted least squares (IRLS) was applied where necessary to account for heteroscedastic uncertainties.

• Covariance handling: full covariance matrices were propagated in the lensing analyses to ensure proper weighting of correlated bins. For rotation curves, uncertainties from distance, inclination, and mass-to-light ratios were included in Monte Carlo resampling.

• Software tools: all analyses were performed using standard open-source libraries (NumPy, SciPy, pandas, matplotlib). Figures and tables were automatically generated with consistent formatting, ensuring one-to-one correspondence with the manuscript.

This pipeline guarantees that results are not tied to a particular software environment and can be replicated independently with the same input data and scripts.

8.3 Reproducibility Assets

To ensure reproducibility, all intermediate and final outputs of the Adaptive-XG analysis have been systematically organized and archived. The assets include:

• Data tables: CSV files containing the results of each stage of the analysis, such as rotation-curve fits (ΔAIC, ΔBIC, χ^2 values), RAR/BTFR summaries, and lensing profiles with covariance matrices.

• Figures: high-resolution plots in PNG and PDF formats, generated directly from the analysis scripts, corresponding to each figure cited in the manuscript.

• Manuscript sections: Word documents containing each chapter and subsection of the paper (Chapters 3–7 and Appendix A), written in a standardized style and with consistent naming conventions.

• Supplementary material: additional files for reproducibility, including example scripts, JSON parameter files, and configuration templates.

All assets are version-controlled and named according to a unified convention, enabling seamless integration into the final manuscript and straightforward verification by independent researchers.

8.4 Open-Science Compliance

Adaptive-XG has been developed with explicit adherence to open-science principles. All datasets employed in this study are publicly available through established astronomical archives (e.g., VizieR, SDSS, ESO), and no proprietary data have been used. This ensures that the analysis is fully transparent and reproducible by independent researchers.

The computational workflow relies exclusively on open-source software libraries (NumPy, SciPy, pandas, matplotlib), and the scripts used to generate figures and tables are organized to allow straightforward replication. By releasing analysis scripts and configuration files alongside the manuscript, the results can be reproduced step-by-step from raw data to final figures.

This compliance with open-science practices ensures that Adaptive-XG is not only an interpretative framework but also a reproducible and verifiable one. The approach lowers barriers for cross-comparison with alternative models and fosters independent validation by the community.

8.5 Reproducibility Summary

The reproducibility framework of Adaptive-XG ensures that all results presented in this manuscript can be independently verified. The use of public datasets, transparent computational pipelines, and openly shared analysis assets eliminates hidden dependencies and guarantees accessibility.

Through systematic organization of data tables, figures, and manuscript sections, combined with adherence to open-science practices, Adaptive-XG stands as a fully testable and reproducible framework.

This commitment to reproducibility strengthens the credibility of the results and enables the community to evaluate, refine, and potentially extend the model. By ensuring that every step from raw data to final figures is transparent, Adaptive-XG aligns with modern standards of scientific integrity and open collaboration.

Chapter 9 – Conclusions

9.1 Summary of Findings

This work has introduced and developed the Adaptive-XG framework as a minimal, scale-dependent extension of general relativity. The central principle of the model is selective activation: modifications emerge only in the low-acceleration regime while GR remains untouched in high-acceleration and strong-field domains.

Rotation curve analyses of the SPARC database demonstrated that Adaptive-XG systematically improves the description of low-surface-brightness and dwarf galaxies, while reverting to GR in high-surface-brightness systems. The framework thus captures the observed diversity of galaxy dynamics without overfitting.

Lensing analyses further supported this picture: stacked cluster profiles (SDSS maxBCG) and galaxy-scale lenses (SLACS, COSMOS, BELLS) showed that GR suffices in high-mass regimes, but Adaptive-XG provides marginal improvements in the outskirts or lower-signal bins. Weak lensing stacks confirmed the same selective activation.

External constraints from Solar System dynamics, pulsar timing, Galactic Center S-star orbits, and EHT black-hole imaging were all satisfied by construction, thanks to the curvature guardrail which suppresses deviations below the 0.5% level in strong fields. The deep-mode extension further showed that curvature invariants are regularized, eliminating classical singularities without spoiling tested predictions.

Finally, robustness analyses confirmed that the framework is stable under parameter variations, ablation of terms, and cross-validation. Together, these results establish Adaptive-XG as a reproducible, predictive, and empirically motivated extension of gravity.

9.2 Scientific Significance

The scientific significance of Adaptive-XG lies in its ability to address galactic-scale anomalies without undermining the remarkable success of general relativity in strong-field and high-acceleration regimes. By construction, the framework is minimal and adaptive: corrections emerge only where observational evidence demands them and remain dormant otherwise.

This selective activation distinguishes Adaptive-XG from both dark-matter based explanations and universal modification schemes. It provides a falsifiable signature that can be tested across independent datasets, making the framework predictive rather than descriptive.

Equally important, Adaptive-XG has been shown to be robust, reproducible, and compliant with open-science standards. Its results are derived from publicly available data, implemented through transparent computational pipelines, and organized in a manner that ensures independent verification.

By combining empirical adequacy, theoretical parsimony, and reproducibility, Adaptive-XG contributes a novel perspective to the ongoing search for a consistent description of gravity across scales. It demonstrates that small, scale-dependent extensions can resolve observational tensions without invoking radical departures from established physics.

9.3 Outlook

Looking forward, Adaptive-XG offers a range of opportunities for further investigation and testing. The imminent arrival of large-scale astronomical surveys—such as Euclid, the Vera C. Rubin Observatory (LSST), and the Nancy Grace Roman Space Telescope—will provide unprecedented datasets of galaxy rotation curves, strong and weak lensing systems, and large-scale structure. These surveys will enable decisive tests of the selective activation principle across diverse environments and redshifts.

Beyond galactic dynamics and lensing, potential applications include the exploration of black-hole merger remnants and gravitational-wave echoes, where curvature-limiting effects may leave subtle imprints. Similarly, the deep-mode regularization of singularities suggests possible relevance to early-Universe cosmology, where limiting curvature could prevent classical divergences at the Big Bang.

In this sense, Adaptive-XG functions not only as a phenomenological patch to GR but also as a conceptual bridge toward more fundamental theories of quantum gravity. By retaining GR's verified predictions while regulating its pathologies, the framework provides a promising avenue for unifying astrophysical observations with theoretical advances.

Acknowledgments

The author gratefully acknowledges the assistance of AI tools (OpenAI's ChatGPT), which were used in drafting, structuring, and formatting portions of this manuscript.

Beyond technical contributions, this work would not have been possible without the enduring support of family. The author expresses heartfelt gratitude to his father, whose intellectual guidance has been a source of inspiration; to his mother, whose encouragement and resilience provided strength; and to his wife, whose companionship and patience sustained this journey. Finally, the deepest thanks go to his daughter, Amethyst, whose presence is a constant reminder of the future generations for whom this research is ultimately intended.

References

Auger, M. W., Treu, T., Bolton, A. S., et al. 2010, ApJ, 724, 511

Bolton, A. S., Burles, S., Koopmans, L. V. E., et al. 2006, ApJ, 638, 703

Capak, P., Aussel, H., Ajiki, M., et al. 2007, ApJS, 172, 99

Chen, Y., Shu, Y., & Bolton, A. S. 2019, ApJ, 881, 8

Event Horizon Telescope Collaboration, Akiyama, K., Alberdi, A., et al. 2019, ApJ, 875, L1

Johnston, D. E., Sheldon, E. S., Tasitsiomi, A., et al. 2007, ApJ, 656, 27

Koester, B. P., McKay, T. A., Annis, J., et al. 2007, ApJ, 660, 239

Lelli, F., McGaugh, S. S., & Schombert, J. M. 2016, AJ, 152, 157

Sheldon, E. S., Johnston, D. E., Scranton, R., et al. 2009, ApJ, 703, 2232

The Dark Energy Survey Collaboration. 2021, Phys. Rev. D, 105, 023520 (DES Y3 results)

de Jong, J. T. A., Verdoes Kleijn, G. A., Erben, T., et al. 2017, A&A, 604, A134 (KiDS DR3)

Will, C. M. 2014, Living Rev. Relativ., 17, 4